# Finite Volume Discretization Preserving Energy Estimates for a Compressible THM Model

Mayssam Mohamad*† Jad Dabaghi‡ Frédéric Grondin† Mazen Saad*

January 2025

**Abstract**

In this work, we investigate a Thermo-Hydro-Mechanical (THM) model describing compressible flow in deformable porous media. Such models play a significant role in various areas of geomechanics, with applications ranging from underground energy storage to oil and gas reservoir engineering. The simulations of THM models are essential for the analysis and design of safe and efficient energy storage cavities. We begin by presenting the mathematical formulation of the model, which consists of a system of parabolic partial differential equations governing the conservation of fluid mass, entropy, and skeleton momentum. First, we derive energy estimates for the compressible model. Next, we focus in particular on the development of numerical discretizations that preserve the energy estimates of the continuous system at the discrete level. To this end, we employ the backward Euler scheme for the time discretization together with the finite volume two-point flux approximation (TPFA) method for the spatial discretization. Numerical experiments are presented to validate the proposed approach and to illustrate its accuracy, efficiency, and robustness.

***Keywords:*** Thermo-Hydro-Mechanical (THM) model; Energy estimates; Compressible flow; Finite volume method.

## 1 Introduction

The rapid deployment of offshore wind farms has increased concerns regarding the management of excess electricity production during peak generation periods. Among the potential solutions, water electrolysis offers a promising solution by converting the excess of renewable electricity during off-peak periods into green hydrogen. The produced hydrogen can be stored in an underwater cemented cavity within a porous geological formation for later use, providing a clean, large-scale, long-term, and potentially cost-effective energy storage solution [15, 28].

However, when hydrogen infiltrates the surrounding construction materials, several complications may occur, such as chemical degradation, alterations in porosity and permeability of the porous medium, structural damage, embrittlement induction, and loss of mechanical strength, each of which may significantly increase the risk of gas leakage [30, 27, 22, 21].

These challenges highlight the need for rigorous mathematical and numerical modeling approaches to capture the coupled physical processes that describe the hydrogen flow and its behavior in porous media, while taking into account the thermal and mechanical effects. Such models provide a framework to evaluate potential risks, such as gas leakage and structural weakening, and to assess different risk mitigation strategies. In this work, we address these issues through numerical simulations based on the finite volume method. Our aim is to establish a robust computational framework that contributes to a safer, more efficient, and more sustainable hydrogen storage.

*Nantes Université, Ecole Centrale Nantes, CNRS, Laboratoire de Mathématiques Jean Leray, LMJL, UMR 6629, F-44000 Nantes, France

†Nantes Université, Ecole Centrale Nantes, CNRS, GeM, UMR 6183, F-44000 Nantes, France

‡Léonard de Vinci Pôle Universitaire, Research Center, 92 916 Paris La Défense, France

Thermo-Hydro-Mechanical (THM) models are essential for analyzing fluid flow in deformable porous materials, as they capture the complex interactions between fluid transport, heat transfer, and mechanical deformations within the subsurface. The theoretical foundation for THM models was initially established by Terzaghi [29], who introduced the effective stress principle, and later generalized by Biot through the theory of poroelasticity [3, 4]. Relying on these pioneering works, a more comprehensive framework for multiphase flows in deformable porous media was developed by Coussy in [10], where the model is reformulated using the first and second principles of thermodynamics. This framework serves as a keystone for the model presented in this work, where small deformations, porosity variations, and linear thermo-poro-elastic behavior of the porous rocks are assumed. In addition, we consider a compressible fluid flow, which represents the main novelty of this study. Compressible flows have been extensively investigated in the context of compositional multiphase flows in porous media, mainly due to their ability to capture the effects of fluid transport in the medium and associated volume changes [8, 26]. Nevertheless, incorporating compressibility within the flow introduces several difficulties into the mathematical model. Indeed, it involves high nonlinearities arising from pressure-dependent density, high computational cost, and potential numerical instabilities due to degeneracies in space and time. The underlying difficulties of such models make their mathematical studies very complex and we mention, for the sake of completeness, the recent contributions [17, 18, 11]. This model consists of three nonlinear partial differential equations modeling the fluid mass conservation equation, the fluid entropy conservation equation, and the skeleton momentum balance equation. This nonlinear and strongly coupled system poses significant analytical and computational challenges, particularly in ensuring stability and energy consistency at the discrete level.

In recent years, an important amount of work has focused on the numerical analysis of THM models. For instance, Droniou et al. [13] studied incompressible single-phase flow in non-fractured deformable porous media, employing the Hybrid Finite Volume (HFV) method [12] combined with the finite element method for the numerical discretization. In the context of fractured porous media, we mention [14, 5] where the authors employed a HFV approach to discretize the flow and heat transfer equations, combined with a finite element approach for the mechanical equation. In contrast, finite volume methods based on the Two-Point Flux Approximation (TPFA) [16] have been widely applied to multiphase flow in rigid porous media, where mechanical deformations are neglected, due to their computational efficiency and conservation properties [25, 18, 1, 6, 2]. While this approach has demonstrated efficiency and accuracy in rigid porous media, its extension to fully coupled THM problems remains challenging, particularly in maintaining energy stability and robustness under large parameter scales.

In the present work, we extend the THM model originally formulated in [10] and previously analyzed for incompressible single-phase flow in [13], to the more realistic case of a compressible fluid, where the density depends on the pressure. To the best of our knowledge, this methodology has never been developed before. A key challenge in this setting is the derivation of energy estimates for the compressible system, due to the additional nonlinearities induced by the pressure-dependant density, and the development of numerical schemes that preserve these estimates at the discrete level.

To this end, we adapt the two-point flux approximation (TPFA) finite volume scheme, commonly employed for multiphase flows in rigid porous media, to the setting of deformable porous materials. The coupled THM system is discretized using the cell-centered finite volume method in space and the implicit backward Euler scheme in time. A particular difficulty arises in the treatment of the discrete density, especially its definition on the interfaces of the mesh, in order to obtain the appropriate energy estimates. This motivates the use of a non-classical formulation to ensure that the discrete scheme inherits the energy stability properties of the continuous model. The proposed definition of the discrete density is also essential for ensuring that the scheme remains consistent with the thermodynamic structure of the continuous model.

Our paper is organized as follows. In Section 2, we present the mathematical model for our problem, where an energy-based reformulation of the entropy conservation equation is also presented. Next, in Section 3, we derive the energy estimates for the continuous model. Furthermore, in Section 4, we introduce the discretization for our system with the implicit Euler scheme in time, and the cell-centered finite volume scheme in space. Then, we demonstrate that the finite volume scheme is equivalent to a discrete variational formulation. Furthermore, the discrete energy estimates are derived in Section 5. Finally, in Section 6, we present some numerical experiments, showing the robustness of our approach. The effects of the skeleton displacement and the fluid compressibility on the numerical solution are also presented in Section 6.

## 2 Thermo-Hydro-Mechanical model

Let $\Omega \subset \mathbb{R}^d$, $d \geq 1$, be an open bounded connected domain representing a porous medium characterised by small strains, displacements, and variations in the porous medium. We denote by $t_F > 0$ the final simulation time and we set $Q_T := (0, t_F) \times \Omega$.

We consider a Thermo-Hydro-Mechanical (THM) model for a non-isothermal, single-phase compressible flow in the porous medium $\Omega$. Linear isotropic thermo-poro-elastic constitutive laws are considered for the skeleton, assuming small variations of temperature around the reference temperature $T_{\text{ref}}$, and thermal equilibrium is assumed between the fluid and the skeleton.

The primary unknowns of the model are the fluid pressure $p$, the temperature $T$, and the displacement of the skeleton $\boldsymbol{u}$. Furthermore, the porous medium is characterized by its porosity $\phi$, which is a nonlinear function, and its absolute permeability tensor denoted by $\mathbb{K}$. Additionally, the viscosity of the fluid is denoted by $\mu$ and the molar density of the gas phase is denoted by $\rho$. The governing system of partial differential equations consists of mass conservation for the fluid, fluid entropy conservation under the assumption of reversible mechanical deformations, and the momentum balance equation for the skeleton. Moreover, we consider homogeneous Neumann boundary conditions for the pressure and temperature variables, and homogeneous Dirichlet boundary conditions for the displacement of the skeleton. The model is described by:

$$\partial_t(\rho(p)\phi(\boldsymbol{u},p,T)) + \operatorname{div}(\rho(p)\boldsymbol{V}(p)) = h_m \qquad \text{in } Q_T, \tag{2.1a}$$

$$\partial_t(S_s + \rho(p)\phi(\boldsymbol{u},p,T)s) + \operatorname{div}\left(\rho(p)s\boldsymbol{V}(p) + \frac{1}{T_{\text{ref}}}\boldsymbol{q}(T)\right) = \frac{h_e}{T} \qquad \text{in } Q_T, \tag{2.1b}$$

$$m_0\partial_{tt}^2\boldsymbol{u} - \operatorname{div}(\boldsymbol{\sigma}(\boldsymbol{u},p,T)) = \boldsymbol{h} \qquad \text{in } Q_T, \tag{2.1c}$$

$$\boldsymbol{\nabla} p\cdot\boldsymbol{n} = 0, \quad \boldsymbol{\nabla} T\cdot\boldsymbol{n} = 0, \quad \boldsymbol{u} = 0 \qquad \text{in } (0,t_F)\times\partial\Omega, \tag{2.1d}$$

$$p(.,0) = p^0, \quad T(.,0) = T^0, \quad \boldsymbol{u}(.,0) = \boldsymbol{u}^0 \qquad \text{in } \Omega, \tag{2.1e}$$

where $S_s$ is the volumetric skeleton entropy, $s$ is the fluid specific entropy, $m_0$ is the specific average fluid-rock density, $h_m$, $h_e$, and $\boldsymbol{h}$ are the source terms and $\boldsymbol{n}$ is the outward normal to $\Omega$.

The Darcy velocity $\boldsymbol{V}$ for the gas phase is defined by

$$\boldsymbol{V} := -\frac{\mathbb{K}}{\mu}\left(\boldsymbol{\nabla} p - \rho \mathrm{g} \boldsymbol{\nabla} \boldsymbol{z}\right), \tag{2.2}$$

where g is the gravitational acceleration constant.

The conductive heat flux $\boldsymbol{q}$ is defined by Fourier's law as

$$\boldsymbol{q} := -\lambda\boldsymbol{\nabla} T, \tag{2.3}$$

where $\lambda$ is the fluid rock average thermal conductivity.

The skeleton's stress is modeled using a linear isotropic thermo-poro-elastic constitutive relation. The symmetric total-stress tensor, $\boldsymbol{\sigma}$, is defined from the effective stress tensor $\boldsymbol{\sigma}^e$ by

$$\begin{aligned}\boldsymbol{\sigma}(\boldsymbol{u},p,T) &:= \boldsymbol{\sigma}^e(\boldsymbol{u}) - bp\mathbb{I}_d - 3\alpha_s K_s(T - T_{\text{ref}})\mathbb{I}_d,\\ \boldsymbol{\sigma}^e(\boldsymbol{u}) &:= \frac{\mathcal{E}}{1+\nu}\left(\boldsymbol{\epsilon}(\boldsymbol{u}) + \frac{\nu}{1-2\nu}\operatorname{div}\boldsymbol{u}\mathbb{I}_d\right),\end{aligned} \tag{2.4}$$

where $\mathcal{E}$ is the effective Young modulus, $\nu$ is the Poisson coefficient, $b$ is the Biot coefficient, $K_s$ is the bulk modulus, and $3\alpha_s$ is the volumetric skeleton thermal dilatation coefficient. In addition, $\boldsymbol{\epsilon}(\boldsymbol{u})$ denotes the strain tensor, defined by $\boldsymbol{\epsilon}(\boldsymbol{u}) := \frac{1}{2}(\boldsymbol{\nabla}\boldsymbol{u} + (\boldsymbol{\nabla}\boldsymbol{u})^\top)$, and $\mathbb{I}_d$ is the $d\times d$ identity matrix. The gradient $\boldsymbol{\nabla}\boldsymbol{u}$ is a matrix in $\mathbb{R}^{d,d}$, with entries given by $(\boldsymbol{\nabla}\boldsymbol{u})_{ij} := \frac{\partial u_i}{\partial x_j}$, for all $1 \leq i,j \leq d$. Moreover, for any matrix $\mathbb{A} \in \mathbb{R}^{d,d}$, the divergence of $\mathbb{A}$ denoted $\operatorname{div}\mathbb{A} \in \mathbb{R}^d$, is the vector defined componentwise by $(\operatorname{div}\mathbb{A})_i := \sum_{k=1}^d \frac{\partial A_{ik}}{\partial x_k}$, for all $1 \leq i \leq d$. We also define the norm of a vector $\boldsymbol{u} \in \mathbb{R}^d$ as $|\boldsymbol{u}| := \left(\sum_{i=1}^d |u_i|^2\right)^{1/2}$.

The porosity $\phi$ and the volumetric skeleton entropy $S_s$ can be modeled as

$$\begin{aligned}\partial_t\phi &= b\partial_t(\operatorname{div}\boldsymbol{u}) - 3\alpha_\phi\partial_t T + \frac{1}{N}\partial_t p,\\ \partial_t S_s &= 3\alpha_s K_s\partial_t(\operatorname{div}\boldsymbol{u}) - 3\alpha_\phi\partial_t p + \frac{C_s}{T_{\text{ref}}}\partial_t T,\end{aligned} \tag{2.5}$$

where $N$ is the Biot modulus, $3\alpha_\phi$ is the volumetric thermal dilatation coefficient related to the porosity, and $C_s$ is the skeleton volumetric heat capacity.

Furthermore, the energy balance in the system is governed by the laws of thermostatics, which relate entropy, energy, and density variations. Specifically, we have the following entropy-energy relation:

$$\partial_t e = T\partial_t s - p\partial_t \left(\frac{1}{\rho}\right), \quad \boldsymbol{\nabla} e = T\boldsymbol{\nabla} s - p\boldsymbol{\nabla}\left(\frac{1}{\rho}\right) \tag{2.6}$$

where $s$ denotes the fluid-specific entropy, $e$ its internal energy, and $\rho$ its density.

Consequently, the entropy conservation equation (2.1b) can be reformulated as:

$$\begin{aligned}&\partial_t(S_s) + \frac{\rho(p)\phi(\boldsymbol{u},p,T)}{T}\partial_t e - \frac{p\phi(\boldsymbol{u},p,T)}{T\rho(p)}\partial_t\rho + \frac{\rho(p)\boldsymbol{V}(p)}{T}\cdot\boldsymbol{\nabla} e - \frac{p\boldsymbol{V}(p)}{T\rho(p)}\cdot\boldsymbol{\nabla}\rho \\ &+ \frac{1}{T_{\text{ref}}}\text{div}q = \frac{h_e}{T} - sh_m.\end{aligned} \tag{2.7}$$

In fact, substituting the fluid entropy-energy relation (2.6) into the entropy conservation equation (2.1b), we obtain:

$$\begin{aligned}&\partial_t S_s(\boldsymbol{u},p,T) + \rho(p)\phi(\boldsymbol{u},p,T)\left(\frac{1}{T}\partial_t e + \frac{p}{T}\partial_t\left(\frac{1}{\rho(p)}\right)\right) + s\partial_t(\rho(p)\phi(\boldsymbol{u},p,T)) \\ &+ s\,\text{div}(\rho(p)\boldsymbol{V}(p)) + \frac{1}{T}\rho(p)\boldsymbol{V}(p)\cdot\left(\boldsymbol{\nabla} e + p\boldsymbol{\nabla}\left(\frac{1}{\rho(p)}\right)\right) \\ &+ \frac{1}{T_{\text{ref}}}\text{div}\boldsymbol{q}(T) = \frac{h_e}{T}.\end{aligned}$$

Moreover, expanding the temporal and spatial derivatives and applying the mass conservation equation (2.1a), we recover the reformulated entropy conservation equation (2.7).

Furthermore, we present some key assumptions on the physical data in order to obtain energy estimates on the system.

**Assumption 1.** **(A1)** *The porosity remains strictly positive i.e. there exists* $\phi_* \in \mathbb{R}_+^*$ *such that* $\phi(\boldsymbol{u},p,T) \geq \phi_* > 0$ *.*

**(A2)** *The energy satisfies* $e(p,T) \geq 0 \quad \forall (p,T) \in \mathbb{R}_+ \times \mathbb{R}_+$ *and the function* $e - Ts$ *is sub-quadratic in the sense that*

$$\lim_{|(p,T)|\to+\infty} \frac{e(p,T) - Ts(p,T)}{|p|^2 + |T|^2} = 0.$$

**(A3)** *The source terms* $h_m$, $\boldsymbol{h}$ *and* $h_e$ *are bounded.*

**(A4)** *The thermo-poro-elastic coefficients satisfy* $C_s > 0$, $\frac{1}{N} > 0$, $\alpha_\phi \geq 0$, $\mathcal{E} > 0$ *and* $\nu \in (0, \frac{1}{2})$.

**(A5)** *There exists a constant* $m_* > 0$ *such that* $m_0 \geq m_* > 0$.

**(A6)** *The density* $\rho(p)$ *is a strictly increasing function and there exists a positive constant* $\gamma$ *such that* $\rho'(p) = \gamma\rho(p)$.

## 3 Energy estimates for the continuous model

In this section, we derive energy estimates for pressure, temperature, displacement, and their respective gradients. To this end, we define the function $g$ by

$$g(p) := \int_0^p \frac{1}{\rho(z)}\,dz. \tag{3.1}$$

Following the notations in [20], we recall that the trace operator $tr : \mathbb{R}^{m,m} \to \mathbb{R}$ is defined by $tr(\mathbb{A}) = \sum_{i=1}^m a_{ii}$, with $\mathbb{A} := (a_{ij})_{1\leq i,j\leq m}$ is a square matrix. The contracted product of two tensors $\mathbb{A}$ and $\mathbb{B}$, both of order $n$, is denoted by $\mathbb{A}\cdot\mathbb{B}$ and defined as the tensor with entries $(\mathbb{A}\cdot\mathbb{B})_{ij} := \sum_{k=1}^{n} a_{ik}b_{kj}$. The double contracted product of $\mathbb{A}$ and $\mathbb{B}$, denoted by $\mathbb{A}:\mathbb{B}$, is a scalar given by $\mathbb{A}:\mathbb{B} := tr\,(\mathbb{A}\cdot\mathbb{B}) = \sum_{i,j=1}^{n} a_{ij}b_{ij}$. For any two vectors $\boldsymbol{v}$ and $\boldsymbol{w}\in\mathbb{R}^m$, we define their tensor product $\boldsymbol{v}\otimes\boldsymbol{w}$ as the $m\times m$ matrix whose $(i,j)$-th entry is given by $(\boldsymbol{v}\otimes\boldsymbol{w})_{ij} := v_i w_j$. Finally, the norm of a tensor $\mathbb{A}$ is denoted by $|\mathbb{A}|$ and is defined by $|\mathbb{A}| := (\mathbb{A}:\mathbb{A})^{1/2}$.

The following lemma provides a key identity that will be used to derive the energy estimates.

**Lemma 1.** *Let $(\boldsymbol{u},p,T)$ be the solution of the system (2.1). We assume that system (2.1) is subject to Neumann boundary conditions for the fluxes and Dirichlet boundary condition for the displacement of the skeleton. We also assume that the gravity vector is equal to $0$. We have the following equality:*

$$\begin{aligned}
&\int_{Q_T} \partial_t E \,\mathrm{d}x\mathrm{d}t + \int_{Q_T} \frac{m_0}{2}\partial_t(|\partial_t\boldsymbol{u}|^2)\,\mathrm{d}x\mathrm{d}t - \int_{Q_T} \phi(\boldsymbol{u},p,T)\frac{\rho'(p)}{\rho(p)}p\partial_t p\,\mathrm{d}x\mathrm{d}t \\
&+ \int_{Q_T} \frac{\mathbb{K}}{\mu}|\boldsymbol{\nabla} p|^2\,\mathrm{d}x\mathrm{d}t + \int_{Q_T} \frac{\lambda}{T_{\mathrm{ref}}}|\boldsymbol{\nabla} T|^2\,\mathrm{d}x\mathrm{d}t + \int_{Q_T} \frac{\mathbb{K}\rho'(p)}{\mu\rho(p)}p|\boldsymbol{\nabla} p|^2\,\mathrm{d}x\mathrm{d}t \\
&= \int_{Q_T} (h_m(g(p)+e-sT) + h_e + \boldsymbol{h}\cdot\partial_t\boldsymbol{u})\,\mathrm{d}x\mathrm{d}t
\end{aligned} \tag{3.2}$$

*where $E$ is the total energy of the system, defined by*

$$\begin{aligned}
E(\boldsymbol{u},p,T) &:= \phi(\boldsymbol{u},p,T)\left(\rho(p)g(p) - p + \rho(p)e\right) + \frac{1}{2}\begin{bmatrix} p & T\end{bmatrix}\mathbb{M}\begin{bmatrix} p \\ T\end{bmatrix} \\
&\quad + \frac{\mathcal{E}}{2(1+\nu)}\left[|\boldsymbol{\epsilon}(\boldsymbol{u})|^2 + \frac{\nu}{1-2\nu}(\mathrm{div}\boldsymbol{u})^2\right],
\end{aligned} \tag{3.3}$$

*where $\mathbb{M}$ denotes a real, symmetric, positive definite matrix defined as*

$$\mathbb{M} := \begin{bmatrix} \frac{1}{N} & -3\alpha_\phi \\ -3\alpha_\phi & \frac{C_s}{T_{\mathrm{ref}}}\end{bmatrix}. \tag{3.4}$$

*Proof.* Multiplying equation (2.1a) by $(g(p)+e)$ then integrating over $Q_T$ and using the divergence theorem, we obtain

$$\begin{aligned}
&\int_{Q_T} \partial_t(\rho(p)\phi(\boldsymbol{u},p,T))g(p)\,\mathrm{d}x\mathrm{d}t + \int_{Q_T} \partial_t(\rho(p)\phi(\boldsymbol{u},p,T))e\,\mathrm{d}x\mathrm{d}t \\
&- \int_{Q_T} \rho(p)\boldsymbol{V}(p)\cdot\boldsymbol{\nabla} g(p)\,\mathrm{d}x\mathrm{d}t - \int_{Q_T} \rho(p)\boldsymbol{V}(p)\cdot\boldsymbol{\nabla} e\,\mathrm{d}x\mathrm{d}t \\
&= \int_{Q_T} h_m(g(p)+e)\,\mathrm{d}x\mathrm{d}t.
\end{aligned} \tag{3.5}$$

Now, multiplying equation (2.7) by $T$ then integrating over $Q_T$ and using the divergence theorem, we obtain

$$\begin{aligned}
&\int_{Q_T} T\partial_t(S_s)\,\mathrm{d}x\mathrm{d}t + \int_{Q_T} \rho(p)\phi(\boldsymbol{u},p,T)\partial_t e\,\mathrm{d}x\mathrm{d}t \\
&- \int_{Q_T} \frac{p\phi(\boldsymbol{u},p,T)}{\rho(p)}\partial_t\rho(p)\,\mathrm{d}x\mathrm{d}t + \int_{Q_T} \rho(p)\boldsymbol{V}(p)\cdot\boldsymbol{\nabla} e\,\mathrm{d}x\mathrm{d}t \\
&- \int_{Q_T} \frac{p\boldsymbol{V}(p)}{\rho(p)}\cdot\boldsymbol{\nabla}\rho(p)\,\mathrm{d}x\mathrm{d}t - \int_{Q_T} \frac{1}{T_{\mathrm{ref}}}\boldsymbol{q}(T)\cdot\boldsymbol{\nabla} T\,\mathrm{d}x\mathrm{d}t \\
&= \int_{Q_T} (h_e - sTh_m)\,\mathrm{d}x\mathrm{d}t.
\end{aligned} \tag{3.6}$$

Finally, multiplying equation (2.1c) by $\partial_t\boldsymbol{u}$ then integrating over $Q_T$ and using the divergence theorem, the definition of the total-stress tensor (2.4) and the fact that $\mathrm{div}(\sigma^e(\boldsymbol{u}))\cdot\partial_t\boldsymbol{u} = -\sigma^e(\boldsymbol{u}) : \epsilon(\partial_t(\boldsymbol{u})) +$

$\mathrm{div}(\epsilon(\boldsymbol{u})\partial_t\boldsymbol{u}) + \frac{\nu}{1-2\nu}\mathrm{div}((\mathrm{div}\boldsymbol{u})(\partial_t\boldsymbol{u}))$, we obtain

$$\begin{aligned}&\int_{Q_T} m_0\partial_{tt}^2\boldsymbol{u}\cdot\partial_t\boldsymbol{u}\,\mathrm{d}x\mathrm{d}t + \int_{Q_T}\sigma^e(\boldsymbol{u}):\epsilon(\partial_t\boldsymbol{u})\,\mathrm{d}x\mathrm{d}t\\ &-\int_{Q_T}(bp+3\alpha_s K_s T)\,\mathrm{div}(\partial_t\boldsymbol{u})\,\mathrm{d}x\mathrm{d}t = \int_{Q_T}\boldsymbol{h}\cdot\partial_t\boldsymbol{u}\,\mathrm{d}x\mathrm{d}t.\end{aligned}\tag{3.7}$$

Moreover, summing equations (3.5), (3.6) and (3.7), we obtain

$$\begin{aligned}&\int_{Q_T}\partial_t(\rho(p)\phi(\boldsymbol{u},p,T))g(p)\,\mathrm{d}x\mathrm{d}t + \int_{Q_T}\partial_t(\rho(p)\phi(\boldsymbol{u},p,T)e)\,\mathrm{d}x\mathrm{d}t\\ &+\int_{Q_T}T\partial_t(S_s)\,\mathrm{d}x\mathrm{d}t - \int_{Q_T}\frac{p\phi(\boldsymbol{u},p,T)}{\rho(p)}\partial_t\rho(p)\,\mathrm{d}x\mathrm{d}t + \int_{Q_T}m_0\partial_{tt}^2\boldsymbol{u}\cdot\partial_t\boldsymbol{u}\,\mathrm{d}x\mathrm{d}t\\ &-\int_{Q_T}\rho(p)\boldsymbol{V}(p)\cdot\boldsymbol{\nabla}g(p)\,\mathrm{d}x\mathrm{d}t - \int_{Q_T}\frac{p\boldsymbol{V}(p)}{\rho(p)}\cdot\boldsymbol{\nabla}\rho(p)\,\mathrm{d}x\mathrm{d}t\\ &-\int_{Q_T}\frac{1}{T_{\mathrm{ref}}}\boldsymbol{q}(T)\cdot\boldsymbol{\nabla}T\,\mathrm{d}x\mathrm{d}t + \int_{Q_T}\sigma^e(\boldsymbol{u}):\epsilon(\partial_t\boldsymbol{u})\,\mathrm{d}x\mathrm{d}t\\ &-\int_{Q_T}(bp+3\alpha_s K_s T)\,\mathrm{div}(\partial_t\boldsymbol{u})\,\mathrm{d}x\mathrm{d}t\\ &=\int_{Q_T}(h_m(g(p)+e-sT)+h_e+\boldsymbol{h}\cdot\partial_t\boldsymbol{u})\mathrm{d}x\mathrm{d}t.\end{aligned}\tag{3.8}$$

Furthermore, from the definition of the function $g$, we have

$$\partial_t(\rho(p)\phi(\boldsymbol{u},p,T))g(p) = \partial_t(\rho(p)\phi(\boldsymbol{u},p,T)g(p)) - \partial_t(\phi(\boldsymbol{u},p,T)p) + p\partial_t\phi.\tag{3.9}$$

In addition, using the chain rule and the identity $v\partial_t v = \frac{1}{2}\partial_t(v^2)$, we obtain:

$$\frac{p\phi(\boldsymbol{u},p,T)}{\rho(p)}\partial_t\rho(p) = \frac{\rho'(p)\phi(\boldsymbol{u},p,T)}{\rho(p)}p\partial_t p.\tag{3.10}$$

Similarly, we have

$$m_0\partial_{tt}^2\boldsymbol{u}\cdot\partial_t\boldsymbol{u} = \frac{m_0}{2}\partial_t(\partial_t\boldsymbol{u}\cdot\partial_t\boldsymbol{u}) = \frac{m_0}{2}\partial_t\left(|\partial_t\boldsymbol{u}|^2\right).\tag{3.11}$$

From the definitions of the Darcy velocity (2.2) and the heat flux (2.3), we have the following equalities:

$$\begin{aligned}\rho(p)\boldsymbol{V}(p)\cdot\boldsymbol{\nabla}g(p) &= -\frac{\mathbb{K}}{\mu}\boldsymbol{\nabla}p\cdot\boldsymbol{\nabla}p,\\ \frac{p\boldsymbol{V}(p)}{\rho(p)}\cdot\boldsymbol{\nabla}\rho(p) &= -\frac{\mathbb{K}\rho'(p)}{\mu\rho(p)}p\boldsymbol{\nabla}p\cdot\boldsymbol{\nabla}p,\\ \frac{1}{T_{\mathrm{ref}}}\boldsymbol{q}(T)\cdot\boldsymbol{\nabla}T &= -\frac{\lambda}{T_{\mathrm{ref}}}\boldsymbol{\nabla}T\cdot\boldsymbol{\nabla}T.\end{aligned}\tag{3.12}$$

From the definition of the effective stress tensor (2.4), we have

$$\sigma^e(\boldsymbol{u}):\epsilon(\partial_t\boldsymbol{u}) = \frac{\mathcal{E}}{2(1+\nu)}\partial_t\left(|\epsilon(\boldsymbol{u})|^2\right) + \frac{\mathcal{E}\nu}{2(1+\nu)(1-2\nu)}\partial_t(\mathrm{div}\boldsymbol{u})^2.\tag{3.13}$$

Consequently, combining (3.9), (3.10), (3.11), (3.12) and (3.13) together with equation (3.8), we obtain

$$\begin{aligned}
&\int_{Q_T} \partial_t \left(\rho(p)\phi(\boldsymbol{u},p,T)g(p) - \phi(\boldsymbol{u},p,T)p + \rho(p)\phi(\boldsymbol{u},p,T)e\right) \mathrm{d}x\mathrm{d}t \\
&+ \int_{Q_T} \frac{m_0}{2}\partial_t\left(|\partial_t \boldsymbol{u}|^2\right) \mathrm{d}x\mathrm{d}t + \int_{Q_T} \frac{\mathcal{E}}{2(1+\nu)}\partial_t\left(|\epsilon(\boldsymbol{u})|^2 + \frac{\nu}{(1-2\nu)}(\mathrm{div}\boldsymbol{u})^2\right) \mathrm{d}x\mathrm{d}t \\
&- \int_{Q_T} \phi(\boldsymbol{u},p,T)\frac{\rho'(p)}{\rho(p)}p\partial_t p \,\mathrm{d}x\mathrm{d}t + \int_{Q_T} \frac{\mathbb{K}}{\mu}|\boldsymbol{\nabla} p|^2 \,\mathrm{d}x\mathrm{d}t + \int_{Q_T} \frac{\lambda}{T_{\mathrm{ref}}}|\boldsymbol{\nabla} T|^2 \,\mathrm{d}x\mathrm{d}t \\
&+ \int_{Q_T} T\partial_t(S_s) + p\partial_t\phi - (bp + 3\alpha_s K_s(T))\,\mathrm{div}(\partial_t\boldsymbol{u}) \,\mathrm{d}x\mathrm{d}t \\
&+ \int_{Q_T} \frac{\mathbb{K}\rho'(p)}{\mu\rho(p)}p|\boldsymbol{\nabla} p|^2 \,\mathrm{d}x\mathrm{d}t = \int_{Q_T} (h_m(g(p)+e-sT) + h_e + \boldsymbol{h}\cdot\partial_t\boldsymbol{u}) \,\mathrm{d}x\mathrm{d}t.
\end{aligned} \tag{3.14}$$

Now, from the definitions of the porosity and skeleton entropy (2.5), we get

$$\begin{aligned}
&T\partial_t(S_s) + p\partial_t\phi - (bp + 3\alpha_s K_s T)\,\mathrm{div}(\partial_t\boldsymbol{u}) \\
&= -3\alpha_\phi p\partial_t T - 3\alpha_\phi T\partial_t p + \frac{1}{2N}\partial_t p^2 + \frac{C_s}{2T_{\mathrm{ref}}}\partial_t T^2 \\
&= \partial_t\left[\frac{1}{2}\begin{bmatrix} p & T\end{bmatrix}\begin{bmatrix} \frac{1}{N} & -3\alpha_\phi \\ -3\alpha_\phi & \frac{C_s}{T_{\mathrm{ref}}}\end{bmatrix}\begin{bmatrix} p \\ T\end{bmatrix}\right].
\end{aligned} \tag{3.15}$$

Now, letting

$$\begin{aligned}
&E(\boldsymbol{u},p,T) := \rho(p)\phi(\boldsymbol{u},p,T)g(p) - \phi(\boldsymbol{u},p,T)p + \rho(p)\phi(\boldsymbol{u},p,T)e \\
&+ \frac{1}{2}\begin{bmatrix} p & T\end{bmatrix}\mathbb{M}\begin{bmatrix} p \\ T\end{bmatrix} + |\epsilon(\boldsymbol{u})|^2 + \frac{\nu}{(1-2\nu)}(\mathrm{div}\boldsymbol{u})^2, \text{ where } \mathbb{M} \text{ is defined by (3.4).}
\end{aligned} \tag{3.16}$$

Then, from equation (3.14), we obtain the desired equality (3.2) which concludes the proof. □

Now, the following result states the energy estimates.

**Proposition 1.** *Let* $(\boldsymbol{u},p,T)$ *be the solution of* (2.1) *and let* $e$ *be the internal energy of the considered system. Assuming that the fluid pressure is positive, the porosity depends on the pressure only, i.e.,* $\phi = \phi(p)$*, and* $\phi_*\gamma$ *is sufficiently small, we obtain the following estimate:*

$$\begin{aligned}
&\|\partial_t\boldsymbol{u}\|_{L^\infty(0,T;L^2(\Omega))} + \|p\|_{L^\infty(0,T;L^2(\Omega))} + \|T\|_{L^\infty(0,T;L^2(\Omega))} + \|e\|_{L^\infty(0,T;L^1(\Omega))} \\
&+ \|\boldsymbol{u}\|_{L^\infty(0,T;H^1(\Omega))} + \|\boldsymbol{\nabla} p\|_{L^2(0,T;L^2(\Omega))} + \|\boldsymbol{\nabla} T\|_{L^2(0,T;L^2(\Omega))} \le C.
\end{aligned} \tag{3.17}$$

*Proof.* Let $y : (0,t_F) \to \mathbb{R}$ be the function defined by

$$y(t) := \int_\Omega \left(E(x,t) + \frac{m_0}{2}|\partial_t\boldsymbol{u}(x,t)|^2 - R(p)\right) \mathrm{d}x,$$

where $R(p)$ is the function defined by

$$R(p) := \int \phi(p)\frac{\rho'(p)}{\rho(p)}p\,dp. \tag{3.18}$$

We aim to show that there exist two functions $k_1 : (0,t_F) \to \mathbb{R}$ and $k_2 : (0,t_F) \to \mathbb{R}$ such that

$$\int_0^{t_F} y'(t)\,\mathrm{d}t \le \int_0^{t_F} (k_1(t) + k_2(t)y(t))\,\mathrm{d}t,$$

in order to apply Gronwall's lemma [19] and thereby derive the desired result.
First, employing the chain rule on $R(p)$, we obtain

$$\partial_t R(p) = \frac{dR}{dp}\partial_t p = \phi(p)\frac{\rho'(p)}{\rho(p)}p\partial_t p. \tag{3.19}$$

Next, from the definition of $y(t)$, employing Lemma 1 and the temporal derivative of $R(p)$ (3.19), and using the assumption that $p \geq 0$, we obtain

$$\int_0^{t_F} y'(t)\,\mathrm{d}t = \int_0^{t_F}\int_\Omega \partial_t E\,\mathrm{d}x\mathrm{d}t + \int_0^{t_F}\int_\Omega \frac{m_0}{2}\partial_t(|\partial_t \boldsymbol{u}|^2)\,\mathrm{d}x\mathrm{d}t$$
$$- \int_0^{t_F}\int_\Omega \partial_t R(p)\,\mathrm{d}x\mathrm{d}t \leq \int_{Q_T} (h_m(g(p)+e-sT) + h_e + \boldsymbol{h}\cdot\partial_t \boldsymbol{u})\,\mathrm{d}x\mathrm{d}t. \tag{3.20}$$

Furthermore, we aim to derive an upper bound for the right-hand side of equation (3.20). Using the assumptions **(A2)** and **(A3)**, we have that there exist positive constants $C_1$, $C_2$, $C_3$ and $C_4 \in \mathbb{R}_+$ such that

$$|h_m| \leq C_1, \quad |h_e| \leq C_2, \quad |\boldsymbol{h}| \leq C_3 \quad \text{and} \quad e - sT \leq C_4(|p|^2 + |T|^2). \tag{3.21}$$

Applying the Cauchy-Schwarz inequality [7], we obtain

$$\int_\Omega \boldsymbol{h}\cdot\partial_t \boldsymbol{u}\,\mathrm{d}x \leq \left(\int_\Omega |\boldsymbol{h}|^2\,\mathrm{d}x\right)^{\frac{1}{2}}\left(\int_\Omega |\partial_t \boldsymbol{u}|^2\,\mathrm{d}x\right)^{\frac{1}{2}} = \|\boldsymbol{h}\|_{L^2(\Omega)}\|\partial_t \boldsymbol{u}\|_{L^2(\Omega)}. \tag{3.22}$$

In addition, since the function $g(p)$ is sublinear, it follows that there exists a constant $C_5 \in \mathbb{R}_+$ such that

$$g(p) \leq C_5 p \quad \text{for all} \quad p \in \mathbb{R}_+. \tag{3.23}$$

Employing inequality (3.22), the bounds (3.21) and (3.23), and applying Young's inequality, we obtain:

$$\begin{aligned}
&\int_{Q_T} (h_m(g(p)+e-sT) + h_e + \boldsymbol{h}\cdot\partial_t \boldsymbol{u})\,\mathrm{d}x\mathrm{d}t \\
&\leq \int_{Q_T} \big(C_1(C_5 p + C_4(|p|^2+|T|^2)) + C_2 + \boldsymbol{h}\cdot\partial_t \boldsymbol{u}\big)\,\mathrm{d}x\mathrm{d}t \\
&\leq C_1C_5\int_{Q_T}\frac{1}{2}\left(|p|^2+1\right)\,\mathrm{d}x\mathrm{d}t + \int_{Q_T} C_1C_4(|p|^2+|T|^2)\,\mathrm{d}x\mathrm{d}t \\
&+ \int_{Q_T} C_2\,\mathrm{d}x\mathrm{d}t + \int_{Q_T}\frac{1}{2}\left(|\boldsymbol{h}|^2 + |\partial_t \boldsymbol{u}|^2\right)\,\mathrm{d}x\mathrm{d}t \\
&\leq \int_{Q_T}\left(C_6(|p|^2+|T|^2) + C_7 + \frac{1}{2}|\partial_t \boldsymbol{u}|^2\right)\,\mathrm{d}x\mathrm{d}t,
\end{aligned} \tag{3.24}$$

where $C_6$ and $C_7$ are two real positive constants such that $C_6 = \max\left(\frac{C_1C_5}{2}, C_1C_4\right)$ and $C_7 = \frac{C_1C_5}{2} + C_2 + \frac{C_3^2}{2}$.

Now, using the fact that $\mathbb{M}$ is a real, symmetric, and positive definite matrix, we have

$$\lambda_{\min}\|(p,T)\|_2^2 \leq \begin{bmatrix} p & T\end{bmatrix}\mathbb{M}\begin{bmatrix} p \\ T\end{bmatrix} \leq \lambda_{\max}\|(p,T)\|_2^2, \tag{3.25}$$

where $\lambda_{\min}, \lambda_{\max} \in \mathbb{R}_+$ are respectively the minimum and the maximum eigenvalues of $\mathbb{M}$.

Furthermore, let us define the function $H : \mathbb{R} \to \mathbb{R}$ by

$$H(p) := \rho(p)g(p) - p \quad \text{where} \quad g(p) := \int_0^p \frac{1}{\rho(z)}\,\mathrm{d}z.$$

The function $H$ verifies $H'(p) = \rho'(p)g(p)$, $H(0) = 0$ and $H(p) \geq 0$ for all $p$.

From assumption 1 **(A1)** and **(A4)**, together with (3.25), the fact that $H(p) \geq 0$ and the definition of $E(\boldsymbol{u}, p, T)$, we obtain:

$$E(\boldsymbol{u},p,T) = \phi(p)\left(\rho(p)g(p) - p + \rho(p)e(p,T)\right) + \frac{1}{2}\begin{bmatrix} p & T\end{bmatrix}\mathbb{M}\begin{bmatrix} p \\ T\end{bmatrix}$$
$$+ \frac{\mathcal{E}}{2(1+\nu)}\left[|\boldsymbol{\epsilon}(\boldsymbol{u})|^2 + \frac{\nu}{1-2\nu}(\mathrm{div}\boldsymbol{u})^2\right] \geq \phi_* H(p) + C_0 e + \frac{1}{2}\lambda_{\min}\|(p,T)\|_2^2.$$

This leads to the following lower bound:

$$C_0(|p|^2 + |T|^2 + e) \le E, \tag{3.26}$$

where $C_0 = \min\left(\frac{1}{2}\lambda_{min}, \rho\phi_*\right) > 0$ is a positive constant.

Employing inequalities (3.24) and (3.26) in equation (3.20), we obtain

$$\begin{aligned}
\int_0^{t_F} y'(t)\,\mathrm{d}t &\le \int_{Q_T} \left( C_6(|p|^2 + |T|^2) + C_7 + \frac{1}{2}|\partial_t \boldsymbol{u}|^2 \right) \mathrm{d}x\mathrm{d}t \\
&\le \int_{Q_T} k_2 \left( E(\boldsymbol{u}, p, T) + \frac{m_0}{2}|\partial_t \boldsymbol{u}|^2 - R(p) \right) \mathrm{d}x\mathrm{d}t \\
&+ \int_{Q_T} \left( C_7 + \frac{1}{2}|\partial_t \boldsymbol{u}|^2 + R(p) \right) \mathrm{d}x\mathrm{d}t \le \int_0^{t_F} \left(k_2 y(t) + k_1\right) \mathrm{d}t,
\end{aligned}$$

where $k_2 = \max\left(\dfrac{C_6}{C_0}, 1\right)$ and $k_1 = C_7|\Omega| + \int_\Omega \left(\frac{1}{2}|\partial_t \boldsymbol{u}|^2 + R(p)\right) \mathrm{d}x$. It follows that

$$y(t_F) \le y(0) + \int_0^{t_F} \left(k_2 y(t) + k_1\right) \mathrm{d}t. \tag{3.27}$$

We now apply Gronwall's Lemma to (3.27). Hence, there exists a constant $C > 0$ such that

$$\int_\Omega \left( E + \frac{m_0}{2}|\partial_t \boldsymbol{u}|^2 - R(p) \right) \mathrm{d}x \le C. \tag{3.28}$$

Furthermore, from Assumption 1, the definition of $R(p)$, and the assumption that $p \ge 0$, we have that $R(p) \ge \phi_*\gamma \int p\,dp = \frac{1}{2}\phi_*\gamma p^2$. Consequently, from (3.28) and the assumption that $\phi_*\gamma$ is sufficiently small, we deduce that $E \in L^\infty(0, t_F; L^1(\Omega))$ and $\partial_t \boldsymbol{u} \in L^\infty(0, t_F; L^2(\Omega))$. Furthermore, using the bound (3.26), we obtain that $p \in L^\infty(0, t_F; L^2(\Omega))$, $T \in L^\infty(0, t_F; L^2(\Omega))$ and $e \in L^\infty(0, t_F; L^1(\Omega))$. Moreover, by the definition of $E(\boldsymbol{u}, p, T)$, and in particular the presence of the term involving $\epsilon(\boldsymbol{u})$, it follows that $\epsilon(\boldsymbol{u}) \in L^\infty(0, t_F; L^2(\Omega))$ and thus $\boldsymbol{\nabla}\boldsymbol{u} \in L^\infty(0, t_F; L^2(\Omega))$. Consequently, we conclude that $\boldsymbol{u} \in L^\infty(0, t_F; H^1(\Omega))$.

In addition, employing equality (3.2), the bound (3.24) together with the assumption that $p \ge 0$ and since $E \in L^\infty(0, t_F; L^1(\Omega))$, $\partial_t \boldsymbol{u} \in L^\infty(0, t_F; L^2(\Omega))$ and $p, T \in L^\infty(0, t_F; L^2(\Omega))$, it follows that

$$\int_\Omega \frac{\mathbb{K}}{\mu} |\boldsymbol{\nabla} p|^2 + \int_\Omega \frac{\lambda}{T_{\text{ref}}} |\boldsymbol{\nabla} T|^2 \,\mathrm{d}x + \int_\Omega \frac{\rho'(p)}{\rho(p)} p\, |\boldsymbol{\nabla} p|^2 \,\mathrm{d}x \le C, \tag{3.29}$$

which implies $\boldsymbol{\nabla} p \in L^2(0, t_F; L^2(\Omega))$ and $\boldsymbol{\nabla} T \in L^2(0, t_F; L^2(\Omega))$. Finally, we conclude the estimate (3.17). □

# 4 Discretization

In this section, we present the discretization of our model. Consequently, we employ the backward Euler scheme in time and the cell-centered two-point flux approximation (TPFA) finite volume scheme in space following [16], [25], [6] and [18]. In the sequel, we consider an isotropic and homogeneous porous medium; for that, we suppose $\mathbb{K} = k\mathbb{I}_d$, where $k$ is a positive constant and $\mathbb{I}_d$ is the identity matrix. We also neglect the gravity term. Moreover, the goal is to show that the energy estimates of section (3) are preserved for the discrete model.

## 4.1 Space and time discretizations

For the time discretization, we employ an implicit Euler scheme. For this purpose, we consider an increasing sequence of points $(t^n)_{0 \le n \le N_T}$ such that $t^0 := 0$ and $t^{N_T} = t_F$, and we introduce the interval $I_n := (t^{n-1}, t^n)$ and the time step $\tau^n := t^n - t^{n-1}$, $1 \le n \le N_T$. For the sake of simplicity, we assume the time step to be constant so that $\tau^n = \delta t > 0$. For a function of time $f$ with sufficient regularity, we denote $f^n := f(t^n)$, $0 \le n \le N_T$, and for $1 \le n \le N_T$, we define the backward differencing operator

$$\partial_t^n f := \frac{f^n - f^{n-1}}{\delta t}.$$

For the space discretization of our model, we consider $\mathcal{T}$ an admissible orthogonal mesh of $\Omega$ called primal mesh such that $\overline{\Omega} = \bigcup_{K\in\mathcal{T}} \overline{K}$ where $K$ are open and convex polygons called control volumes. We denote by $\mathcal{E}_h$ the set of mesh edges. Boundary edges are collected in the set $\mathcal{E}_h^{\mathrm{ext}} := \{\sigma \in \mathcal{E}_h;\, \sigma \subset \partial\Omega\}$ and internal edges are collected in the set $\mathcal{E}_h^{\mathrm{int}} = \mathcal{E}_h \setminus \mathcal{E}_h^{\mathrm{ext}}$. Likewise, the edges of an element $K \in \mathcal{T}$ are collected in the set $\mathcal{E}_K$, and the latter is decomposed into interior edges $\mathcal{E}_K^{\mathrm{int}}$ and boundary edges $\mathcal{E}_K^{\mathrm{ext}}$. For all $K \in \mathcal{T}$, we denote by $\boldsymbol{x}_K$ the cell center of $K$ and $\mathcal{N}(K)$ the set of its neighbors defined as

$$\mathcal{N}(K) := \{L \in \mathcal{T}; \exists\, \sigma_{KL} \in \mathcal{E}_K,\, \sigma_{KL} = \overline{K} \cap \overline{L}\} = \mathcal{N}_{\mathrm{int}}(K) \cup \mathcal{N}_{\mathrm{ext}}(K),$$

where $\mathcal{N}_{\mathrm{int}}(K)$ is the set of neighbors of $K$ located in the interior of $\mathcal{T}$ and $\mathcal{N}_{\mathrm{ext}}(K)$ is the set of edges of $K$ on the boundary $\partial\Omega = \partial K \cap \partial\Omega$ . For an edge $\sigma_{KL} \in \mathcal{E}_K$ shared by two elements $K$ and $L$, we define the distance between these elements $d_{KL} := \mathrm{dist}(\boldsymbol{x}_K, \boldsymbol{x}_L)$ and $\tau_{KL} := \dfrac{|\sigma_{KL}|}{d_{KL}}$ as the transmissibility coefficient through $\sigma_{KL}$.

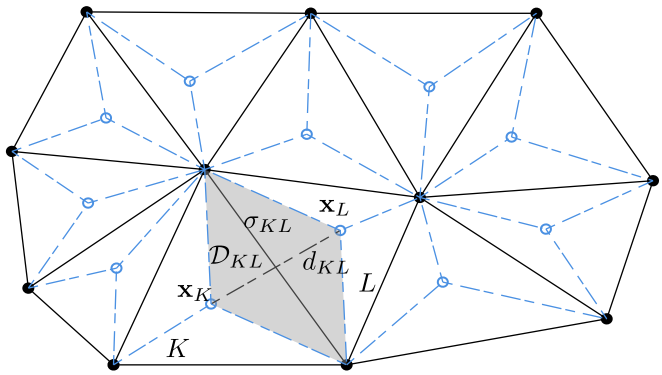


Figure 1: Illustration of the primal and dual meshes

To discretize our unknowns, we introduce the discrete space of cellwise constant functions as follows

$$L_h := \left\{ v_h \in L^2(\Omega),\, v_h|_K = v_K\, \forall K \in \mathcal{T} \right\}.$$

We also define the scalar product on the space $L_h$ and its underlying norm by

$$(w_h, v_h)_{L_h(\Omega)} := \sum_{K\in\mathcal{T}} |K| w_K v_K, \quad \text{and} \quad \|v_h\|_{L_h(\Omega)} := \left( \sum_{K\in\mathcal{T}} |K||v_K|^2 \right)^{\frac{1}{2}}.$$

Moreover, we construct the dual diamond cell upon the interface $\sigma_{KL}$ as the polygonal domain having $\boldsymbol{x}_K$ and $\boldsymbol{x}_L$ as vertices. We denote it by $\mathcal{D}_{KL}$ (Figure 1 provides a quick illustration). The $d$-dimensional measure $|\mathcal{D}_{KL}|$ of $\mathcal{D}_{KL}$ is given by

$$|\mathcal{D}_{KL}| := \frac{1}{d} |\sigma_{KL}| d_{KL}.$$

We associate a diamond $\mathcal{D}_{KL}$ on each interface $\sigma_{KL}$ when the two elements $K$ and $L$ exist, and in the case where $\sigma \subset \partial\Omega$, we associate a half diamond denoted by $\mathcal{D}_{K\sigma}$. We also denote

$$\mathcal{D}_{\mathrm{int}} := \{\mathcal{D}_{KL}, K \in \mathcal{T} \text{and}\, L \in \mathcal{N}(K)\}, \quad \mathcal{D}_{\mathrm{ext}} := \{\mathcal{D}_{K\sigma}, K \in \mathcal{T} \text{and}\, \sigma \in \mathcal{E}_K^{\mathrm{ext}}\}.$$

Then, we have

$$\overline{\Omega} = \mathcal{D}_{\mathrm{int}} \cup \mathcal{D}_{\mathrm{ext}},$$

and the mesh composed of the diamonds is called the dual mesh.

For a piecewise constant function $v_h \in L_h$ defined per control volume, we define on the dual mesh the discrete broken gradient $\boldsymbol{\nabla}_h v_h \in \mathbb{R}^d$ as a constant per diamond by

$$\boldsymbol{\nabla}_h v_h(x) := \begin{cases} d\frac{v_L - v_K}{d_{KL}} \boldsymbol{n}_{KL} & \text{if } \boldsymbol{x} \in \mathcal{D}_{KL}, \\ d\frac{v_\sigma - v_K}{d_{K\sigma}} \boldsymbol{n}_{K\sigma} & \text{if } \boldsymbol{x} \in \mathcal{D}_{K\sigma}. \end{cases} \tag{4.1}$$

Analogously, for a piecewise constant vector function $\boldsymbol{w}_h \in L_h^d$ defined per control volume, we define on the dual mesh the discrete broken gradient $\boldsymbol{\nabla}_h \boldsymbol{w}_h \in \mathbb{R}^{d\times d}$ by

$$\boldsymbol{\nabla}_h \boldsymbol{w}_h(x) := \begin{cases} d\frac{\boldsymbol{w}_L - \boldsymbol{w}_K}{d_{KL}} \otimes \boldsymbol{n}_{KL} & \text{if } \boldsymbol{x} \in \mathcal{D}_{KL}, \\ d\frac{\boldsymbol{w}_\sigma - \boldsymbol{w}_K}{d_{K\sigma}} \otimes \boldsymbol{n}_{K\sigma} & \text{if } \boldsymbol{x} \in \mathcal{D}_{K\sigma}. \end{cases} \tag{4.2}$$

When there is no confusion, we write $\sum_{\sigma_{KL} \in \mathcal{E}_h}$ to be the sum over all diamonds, including the diamonds associated with interfaces on the boundary of the domain.

Furthermore, for $(w_h, v_h) \in (L_h)^2$, we define the discrete $H_0^1$ inner product as follows:

$$\langle w_h, v_h \rangle_{H_h(\Omega)} := d \sum_{\sigma_{KL} \in \mathcal{E}_h} \frac{|\sigma_{KL}|}{d_{KL}} (w_L - w_K)(v_L - v_K),$$

and the corresponding discrete $H_0^1$ norm as $\|v_h\|_{H_h(\Omega)} := \left(\langle v_h, v_h \rangle_{H_h(\Omega)}\right)^{1/2} = \left(d \sum_{\sigma_{KL} \in \mathcal{E}_h} \frac{|\sigma_{KL}|}{d_{KL}} (v_L - v_K)^2\right)^{1/2}$. In addition, the norm $\|v_h\|_{H_h}$ coincides with the $L^2(\Omega)$ norm of $\boldsymbol{\nabla}_h v_h$. In fact

$$\begin{aligned} \|\boldsymbol{\nabla}_h v_h\|^2_{L^2(\Omega)} &= \int_\Omega |\boldsymbol{\nabla}_h v_h|^2 \,\mathrm{d}x = \sum_{\sigma_{KL} \in \mathcal{E}_h} \int_{\mathcal{D}_{KL}} |\boldsymbol{\nabla}_h v_h|^2 \mathrm{d}x \\ &= d \sum_{\sigma_{KL} \in \mathcal{E}_h} \frac{|\sigma_{KL}|}{d_{KL}} |v_L - v_K|^2 := \|v_h\|^2_{H_h}. \end{aligned}$$

Additionally, we assimilate a discrete field $\boldsymbol{G}_{KL}$ to the diamond piecewise constant vector function

$$\boldsymbol{G}_h = \sum_{\sigma_{KL} \in \mathcal{E}_h} \boldsymbol{G}_{KL} \mathbb{1}_{\mathcal{D}_{KL}}.$$

where $\mathbb{1}_{\mathcal{D}_{KL}}$ is the indicator function of the set $\mathcal{D}_{KL}$. Moreover, we define the discrete divergence of the vector field $\boldsymbol{G}_h$ by

$$\mathrm{div}_h \boldsymbol{G}_h := \frac{1}{|K|} \sum_{L \in \mathcal{N}(K)} |\sigma_{KL}| \boldsymbol{G}_h \cdot \boldsymbol{n}_{KL}. \tag{4.3}$$

## 4.2 The finite volume scheme

The finite volume scheme is obtained by writing the balance equations on each control volume. First, we discretize the mass conservation equation (2.1a). Let $K \in \mathcal{T}$. By integrating over $[t^{n-1}, t^n] \times K$ and using the divergence theorem, we obtain

$$\begin{aligned} &\int_K ((\rho(p)\phi(\boldsymbol{u}, p, T))(t^n, x) - (\rho(p)\phi(\boldsymbol{u}, p, T))(t^{n-1}, x))dx \\ &+ \delta t \int_{t^{n-1}}^{t^n} \int_{\partial K} \rho(p) \boldsymbol{V}(p) \cdot \mathbf{n} \, d\sigma dt = \delta t \int_{t^{n-1}}^{t^n} \int_K h_m(x, t) \, dx dt. \end{aligned} \tag{4.4}$$

The resulting equation is discretized with an implicit Euler scheme in time, and the normal gradients are discretized with a centered finite difference scheme, then for $n = 1, \ldots, N_T$, (4.4) reads

$$\begin{aligned} &|K| \left(\rho(p_K^n)\phi(\boldsymbol{u}_K^n, p_K^n, T_K^n) - \rho(p_K^{n-1})\phi(\boldsymbol{u}_K^{n-1}, p_K^{n-1}, T_K^{n-1})\right) \\ &+ \delta t \sum_{L \in \mathcal{N}(K)} \mathcal{F}_{1,KL}(p^n) = \delta t |K| h^n_{m,K}. \end{aligned} \tag{4.5}$$

Here, the discrete elementwise source term $h^n_{m,K}$ is defined by

$$h^n_{m,K} := \int_{I_n} \frac{1}{|K|\delta t} \left( \int_K h_m(x,t)\, dx \right)(t)\, dt.$$

Furthermore, the total flux across $\sigma_{KL} \in \mathcal{E}_h^{\text{int}}$, $\sigma_{KL} = \partial K \cap \partial L$, is defined by

$$\mathcal{F}_{1,KL}(p^n) := \rho^n_{KL} \frac{k}{\mu} \tau_{KL} \left( p^n_K - p^n_L \right),$$

where $\rho^n_{KL}$ is the mean value of the density, and it is defined by,

$$\frac{1}{\rho^n_{KL}} := \begin{cases} \dfrac{1}{p^n_K - p^n_L} \displaystyle\int_{p^n_L}^{p^n_K} \frac{1}{\rho(z)} dz & \text{if} \quad p^n_K \neq p^n_L, \\ \frac{1}{\rho^n_K} & \text{otherwise.} \end{cases} \tag{4.6}$$

We observe that the numerical flux $\mathcal{F}_{1,KL}(p^n)$ is conservative in the sense that,

$$\mathcal{F}_{1,LK}(p^n) = -\mathcal{F}_{1,KL}(p^n).$$

Next, we discretize the energy conservation equation (2.1b). Let $K \in \mathcal{T}$. By integrating over $[t^{n-1}, t^n] \times K$, using the divergence theorem and an implicit Euler scheme in time. Then, for $n = 1, \dots, N_T$, we obtain

$$\begin{aligned} &|K| \left( S^n_{s,K} + \rho^n_K \phi^n_K s^n_K - S^{n-1}_{s,K} - \rho^{n-1}_K \phi^{n-1}_K s^{n-1}_K \right) \\ &+ \delta t \sum_{L \in \mathcal{N}(K)} \mathcal{F}_{2,KL}(p^n, T^n) = \delta t |K| \frac{h^n_{e,K}}{T^n_K}. \end{aligned} \tag{4.7}$$

Here, for $L \in \mathcal{N}(K)$, we have

$$\mathcal{F}_{2,KL}(p^n, T^n) := \rho^n_{KL} s^n_{KL} \frac{k}{\mu} \tau_{KL} \left( p^n_K - p^n_L \right) + \frac{\lambda}{T_{\text{ref}}} \tau_{KL} \left( T^n_K - T^n_L \right),$$

with

$$s^n_{KL} := \frac{s^n_K + s^n_L}{2}.$$

Furthermore, the discrete elementwise source term $h^n_{e,K}$ is defined by

$$h^n_{e,K} := \int_{I_n} \frac{1}{|K|\delta t} \left( \int_K h_e(x,t)\, dx \right)(t)\, dt.$$

We observe that $\mathcal{F}_{2,LK}(p^n, T^n) = -\mathcal{F}_{2,KL}(p^n, T^n)$, which provides a conservative numerical approximation.

Now, we discretize the momentum conservation equation (2.1c). Let $K \in \mathcal{T}$. By integrating over $[t^{n-1}, t^n] \times K$ and using the divergence theorem together with the definition of the total-stress tensor (2.4), we obtain

$$\begin{aligned} &\int_K m_0 \left( \partial_t \boldsymbol{u}(t^n, x) - \partial_t \boldsymbol{u}(t^{n-1}, x) \right) dx \\ &- \delta t \int_{\partial K} \frac{\mathcal{E}}{1+\nu} \left( \boldsymbol{\epsilon}(\boldsymbol{u}^n) + \frac{\nu}{1-2\nu} \text{div} \boldsymbol{u}^n \mathbb{I}_d \right) \boldsymbol{n}\, d\sigma \\ &+ \delta t \int_{\partial K} \left( b p^n \mathbb{I}_d + 3\alpha_s K_s (T^n - T_{\text{ref}}) \mathbb{I}_d \right) \boldsymbol{n}\, d\sigma = \delta t \int_{t^{n-1}}^{t^n} \int_K \boldsymbol{h}\, dx \text{d}t. \end{aligned} \tag{4.8}$$

Furthermore, we have

$$
\begin{aligned}
&\int_{\partial K} \epsilon(\boldsymbol{u}^n)\boldsymbol{n}\, d\sigma = \sum_{L\in\mathcal{N}_{\text{int}}(K)} \int_{\sigma_{KL}} \epsilon(\boldsymbol{u}^n)\boldsymbol{n}_{KL}\, d\sigma + \sum_{\sigma\in\mathcal{N}_{\text{ext}}(K)} \int_{\sigma_{K\sigma}} \epsilon(\boldsymbol{u}^n)\boldsymbol{n}_{K\sigma}\, d\sigma \\
&= \sum_{L\in\mathcal{N}_{\text{int}}(K)} \int_{\sigma_{KL}} \frac{1}{2}\left(\boldsymbol{\nabla}\boldsymbol{u}^n + (\boldsymbol{\nabla}\boldsymbol{u}^n)^\top\right)\boldsymbol{n}_{KL}\, d\sigma \\
&+ \sum_{\sigma\in\mathcal{N}_{\text{ext}}(K)} \int_{\sigma_{K\sigma}} \frac{1}{2}\left(\boldsymbol{\nabla}\boldsymbol{u}^n + (\boldsymbol{\nabla}\boldsymbol{u}^n)^\top\right)\boldsymbol{n}_{K\sigma}\, d\sigma \\
&= \frac{1}{2}\sum_{L\in\mathcal{N}(K)} \tau_{KL}\left(\left([\boldsymbol{u}_L^n - \boldsymbol{u}_K^n]\otimes\boldsymbol{n}_{KL}\right)\boldsymbol{n}_{KL} + \left([\boldsymbol{u}_L^n - \boldsymbol{u}_K^n]\otimes\boldsymbol{n}_{KL}\right)^\top\boldsymbol{n}_{KL}\right).
\end{aligned}
\tag{4.9}
$$

In the same way, we have

$$
\begin{aligned}
&\int_{\partial K} (\operatorname{div}(\boldsymbol{u}^n)\mathbb{I}_d)\boldsymbol{n}\, d\sigma \\
&= \sum_{L\in N_{\text{int}}(K)} \int_{\sigma_{KL}} (\operatorname{div}(\boldsymbol{u}^n)\mathbb{I}_d)\boldsymbol{n}_{KL}\, d\sigma + \sum_{\sigma\in N_{\text{ext}}(K)} \int_{\sigma_{K\sigma}} (\operatorname{div}(\boldsymbol{u}^n)\mathbb{I}_d)\boldsymbol{n}_{K\sigma}\, d\sigma \\
&= \sum_{L\in N_{\text{int}}(K)} |\sigma_{KL}|(\operatorname{div}(\boldsymbol{u}^n)\mathbb{I}_d)_{KL}\boldsymbol{n}_{KL} + \sum_{\sigma\in N_{\text{ext}}(K)} |\sigma_{K\sigma}|(\operatorname{div}(\boldsymbol{u}^n)\mathbb{I}_d)_{K\sigma}\boldsymbol{n}_{K\sigma} \\
&= \sum_{L\in\mathcal{N}(K)} |\sigma_{KL}|(\operatorname{div}(\boldsymbol{u}^n)\mathbb{I}_d)_{KL}\boldsymbol{n}_{KL},
\end{aligned}
\tag{4.10}
$$

where $(\operatorname{div}(\boldsymbol{u}^n)\mathbb{I}_d)_{KL} := \dfrac{(\operatorname{div}(\boldsymbol{u}^n)\mathbb{I}_d)_K + (\operatorname{div}(\boldsymbol{u}^n)\mathbb{I}_d)_L}{2}$ and the ij-entry of the matrix $(\operatorname{div}(\boldsymbol{u}^n)\mathbb{I}_d)_K$ is defined by

$$((\operatorname{div}(\boldsymbol{u}^n)\mathbb{I}_d)_K)_{ij} := \operatorname{div}_K\boldsymbol{u}^n(\mathbb{I}_d)_{ij},$$

with $\operatorname{div}_K\boldsymbol{u}^n$ being the discrete divergence of $\boldsymbol{u}^n$ defined by (4.3).

Moreover, using the backward differencing operator, equation (4.8) reads

$$|K|\frac{\boldsymbol{u}_K^n + \boldsymbol{u}_K^{n-2} - 2\boldsymbol{u}_K^{n-1}}{\delta t} + \delta t\sum_{L\in\mathcal{N}(K)} \mathcal{F}_{3,KL}(\boldsymbol{u}^n, p^n, T^n) = \delta t|K|\boldsymbol{h}_K^n. \tag{4.11}$$

Here, employing (4.9) and (4.10), we have

$$
\begin{aligned}
&\mathcal{F}_{3,KL}(\boldsymbol{u}^n, p^n, T^n) := \\
&\frac{\mathcal{E}}{(1+\nu)}\frac{\tau_{KL}}{2}\left[\left((\boldsymbol{u}_K^n - \boldsymbol{u}_L^n)\otimes\boldsymbol{n}_{KL}\right)\boldsymbol{n}_{KL} + \left[(\boldsymbol{u}_K^n - \boldsymbol{u}_L^n)\otimes\boldsymbol{n}_{KL}\right]^\top\boldsymbol{n}_{KL}\right] \\
&- \frac{\mathcal{E}\nu}{(1+\nu)(1-2\nu)}|\sigma_{KL}|\left(\operatorname{div}\boldsymbol{u}^n\mathbb{I}_d\right)_{KL}\boldsymbol{n}_{KL} + b|\sigma_{KL}|p_{KL}^n\mathbb{I}_d\boldsymbol{n}_{KL} \\
&+ |\sigma_{KL}|3\alpha_s K_s\left(T_{KL}^n - T_{\text{ref}}\right)\mathbb{I}_d\boldsymbol{n}_{KL}
\end{aligned}
$$

where

$$(\operatorname{div}\boldsymbol{u}^n\mathbb{I}_d)_{KL} := \frac{\operatorname{div}_K\boldsymbol{u}^n + \operatorname{div}_L\boldsymbol{u}^n}{2}\mathbb{I}_d,\ \ p_{KL}^n := \frac{p_K^n + p_L^n}{2},\ \ T_{KL}^n := \frac{T_K^n + T_L^n}{2}.$$

Furthermore, the discrete elementwise source term $\boldsymbol{h}_K^n$ is defined by

$$\boldsymbol{h}_K^n := \int_{I_n} \frac{1}{|K|\delta t}\left(\int_K \boldsymbol{h}(x,t)\, dx\right)(t)\, dt.$$

We observe that $\mathcal{F}_{3,KL}(\boldsymbol{u}^n, p^n, T^n) = -\mathcal{F}_{3,LK}(\boldsymbol{u}^n, p^n, T^n)$ which provides a conservative numerical approximation.

Integrating the porosity and skeleton entropy equations (2.5) over $[t^{n-1}, t^n] \times K$, using the divergence theorem together with the discrete divergence definition (4.3). Then, the discrete porosity $(\phi_h^n)_{n=1,\dots,N_T}$ and skeleton entropy $(S_{s,h}^n)_{n=1,\dots,N_T}$ are given by

$$\begin{aligned} \frac{\phi_h^n - \phi_h^{n-1}}{\delta t} &= b\, \mathrm{div}_K \partial_t^n \boldsymbol{u} - 3\alpha_\phi \frac{T_h^n - T_h^{n-1}}{\delta t} + \frac{1}{N} \frac{p_h^n - p_h^{n-1}}{\delta t}, \\ \frac{S_{s,h}^n - S_{s,h}^{n-1}}{\delta t} &= 3\alpha_s K_s\, \mathrm{div}_K \partial_t^n \boldsymbol{u} - 3\alpha_\phi \frac{p_h^n - p_h^{n-1}}{\delta t} + \frac{C_s}{T_{\mathrm{ref}}} \frac{T_h^n - T_h^{n-1}}{\delta t}. \end{aligned} \tag{4.12}$$

Furthermore, we discretize the energy-entropy relation (2.6). Let $K \in \mathcal{T}$. By integrating the first equation of (2.6) over $[t^{n-1}, t^n] \times K$, we obtain

$$s_K^n - s_K^{n-1} = \frac{1}{T_K^n} \left( e_K^n - e_K^{n-1} \right) + \frac{p_K^n}{T_K^n} \left( \frac{1}{\rho_K^n} - \frac{1}{\rho_K^{n-1}} \right). \tag{4.13}$$

Let $\psi \in H^1(\Omega)$ be a test function. Multiplying the second equation of (2.6) by $\rho\psi$ and applying the divergence operator to both sides, we obtain:

$$\mathrm{div} \left( \rho\psi \boldsymbol{\nabla} s \right) = \mathrm{div} \left( \frac{\rho\psi}{T} \boldsymbol{\nabla} e \right) + \mathrm{div} \left( \frac{p\rho\psi}{T} \boldsymbol{\nabla} \left( \frac{1}{\rho} \right) \right). \tag{4.14}$$

Let $K \in \mathcal{T}$. By integrating equation (4.14) over $[t^{n-1}, t^n] \times K$ and using the divergence theorem, we obtain

$$\begin{aligned} \sum_{L \in \mathcal{N}(K)} \rho_{KL}^n \psi_{KL} \tau_{KL} (s_L^n - s_K^n) &= \sum_{L \in \mathcal{N}(K)} \frac{\tau_{KL} \rho_{KL}^n \psi_{KL}}{T_{KL}^n} (e_L^n - e_K^n) \\ &+ \sum_{L \in \mathcal{N}(K)} \tau_{KL} \frac{p_{KL}^n \rho_{KL}^n \psi_{KL}}{T_{KL}^n} \left( \frac{1}{\rho_L^n} - \frac{1}{\rho_K^n} \right) \end{aligned} \tag{4.15}$$

where $T_{KL}^n := \dfrac{T_K^n + T_L^n}{2}$, $p_{KL}^n := \dfrac{p_K^n + p_L^n}{2}$, $\psi_{KL} := \dfrac{\psi_K + \psi_L}{2}$ and $\rho_{KL}$ is defined by (4.6).

Finally, at every time step $1 \le n \le N_T$, we are looking for $\boldsymbol{\mathcal{U}}_h^n = (\boldsymbol{u}_h^n, p_h^n, T_h^n) \in \mathbb{R}^{(2+d)|\mathcal{T}_h|}$ a solution to the nonlinear system of algebraic equations (4.5), (4.7) and (4.11).

We aim to show that the finite volume scheme (4.5)–(4.11) can be reformulated as a discrete variational formulation. To this end, we recall the discrete integration by parts formula [25] and we introduce a key identity.

**Lemma 2** (Discrete integration by parts formula [24, Lemma 4.3.2])**.** *Let $\Omega$ be an open bounded polygonal subset of $\mathbb{R}^d$, $\mathcal{T}$ an admissible finite volume mesh in the sense given in Section 4.1. Let $F_{KL}$, $K \in \mathcal{T}$ and $L \in \mathcal{N}(K)$ be a value in $\mathbb{R}$ depending on $K$ and $L$ such that $F_{KL} = -F_{LK}$ (anti-symmetric), and let $\varphi$ be a function which is constant on each cell $K \in \mathcal{T}$, that is, $\varphi(\boldsymbol{x}) = \varphi_K$ if $\boldsymbol{x} \in K$. Then*

$$\sum_{K \in \mathcal{T}} \sum_{L \in \mathcal{N}(K)} F_{KL} \varphi_K = - \sum_{\sigma_{KL} \in \mathcal{E}_h} F_{KL} (\varphi_L - \varphi_K) = -\frac{1}{2} \sum_{K \in \mathcal{T}} \sum_{L \in \mathcal{N}(K)} F_{KL} (\varphi_L - \varphi_K). \tag{4.16}$$

**Proposition 2.** *Let $\psi_h \in H_h$. We have the identity:*

$$\begin{aligned} &\sum_{K \in \mathcal{T}} \sum_{L \in \mathcal{N}(K)} \rho_{KL}^n (s_L^n - s_K^n) \frac{k}{\mu} \tau_{KL} \left( p_L^n - p_K^n \right) \psi_K \\ &= \sum_{K \in \mathcal{T}} \sum_{L \in \mathcal{N}(K)} \frac{k}{\mu} \frac{\tau_{KL} \rho_{KL}^n}{T_{KL}^n} \left( (e_L^n - e_K^n) + p_{KL}^n \left( \frac{1}{\rho_L^n} - \frac{1}{\rho_K^n} \right) \right) (p_L^n - p_K^n) \psi_{KL}. \end{aligned}$$

*Proof.* Starting with the left-hand side. Reorganizing the sum by edges, using the fact that $\rho_{KL}^n (s_L^n - s_K^n) \tau_{KL} \left( p_L^n - p_K^n \right)$ is symmetric, then reorganizing the sum on edges per cell, we obtain

$$\begin{aligned} &\sum_{K \in \mathcal{T}} \sum_{L \in \mathcal{N}(K)} \rho_{KL}^n (s_L^n - s_K^n) \frac{k}{\mu} \tau_{KL} \left( p_L^n - p_K^n \right) \psi_K \\ &= \frac{1}{2} \sum_{K \in \mathcal{T}} \sum_{L \in \mathcal{N}(K)} \rho_{KL}^n (s_L^n - s_K^n) \frac{k}{\mu} \tau_{KL} \left( p_L^n - p_K^n \right) (\psi_K + \psi_L). \end{aligned} \tag{4.17}$$

Furthermore, since $\rho_{KL}^n(s_L^n - s_K^n)\tau_{KL}(\psi_K + \psi_L)$ is antisymmetric, we apply the discrete integration by parts Lemma 2 to obtain

$$\begin{aligned}&\frac{1}{2}\sum_{K\in\mathcal{T}}\sum_{L\in\mathcal{N}(K)} \rho_{KL}^n(s_L^n - s_K^n)\frac{k}{\mu}\tau_{KL}\left(p_L^n - p_K^n\right)\left(\psi_K + \psi_L\right)\\&= 2\sum_{K\in\mathcal{T}}\sum_{L\in\mathcal{N}(K)} \rho_{KL}^n(s_K^n - s_L^n)\frac{k}{\mu}\tau_{KL}\psi_{KL}p_K^n, \text{ with } \psi_{KL} := \frac{\psi_K + \psi_L}{2}.\end{aligned}\tag{4.18}$$

Now, substituting the discrete entropy-energy relation (4.15) in equation (4.18), we obtain

$$\begin{aligned}&2\sum_{K\in\mathcal{T}}\sum_{L\in\mathcal{N}(K)} \rho_{KL}^n(s_K^n - s_L^n)\frac{k}{\mu}\tau_{KL}\psi_{KL}p_K^n\\&= 2\sum_{K\in\mathcal{T}}\frac{k}{\mu}\times\\&\left(\sum_{L\in\mathcal{N}(K)}\frac{\tau_{KL}\rho_{KL}^n\psi_{KL}}{T_{KL}^n}(e_K^n - e_L^n) + \sum_{L\in\mathcal{N}(K)}\tau_{KL}\frac{p_{KL}^n\rho_{KL}^n\psi_{KL}}{T_{KL}^n}\left(\frac{1}{\rho_K^n} - \frac{1}{\rho_L^n}\right)\right)p_K^n.\end{aligned}\tag{4.19}$$

Applying the discrete integration by parts Lemma 2, since $\frac{\tau_{KL}\rho_{KL}^n\psi_{KL}}{T_{KL}^n}(e_K^n - e_L^n)$ and $\tau_{KL}\frac{p_{KL}^n\rho_{KL}^n\psi_{KL}}{T_{KL}^n}\left(\frac{1}{\rho_K^n} - \frac{1}{\rho_L^n}\right)$ are antisymmetric, we obtain

$$\begin{aligned}&2\sum_{K\in\mathcal{T}}\frac{k}{\mu}\left(\sum_{L\in\mathcal{N}(K)}\frac{\tau_{KL}\rho_{KL}^n\psi_{KL}}{T_{KL}^n}(e_K^n - e_L^n) + \sum_{L\in\mathcal{N}(K)}\tau_{KL}\frac{p_{KL}^n\rho_{KL}^n\psi_{KL}}{T_{KL}^n}\left(\frac{1}{\rho_K^n} - \frac{1}{\rho_L^n}\right)\right)p_K^n\\&= \sum_{K\in\mathcal{T}}\sum_{L\in\mathcal{N}(K)}\frac{k}{\mu}\frac{\tau_{KL}\rho_{KL}^n\psi_{KL}}{T_{KL}^n}(e_L^n - e_K^n)(p_L^n - p_K^n)\\&+ \sum_{K\in\mathcal{T}}\sum_{L\in\mathcal{N}(K)}\frac{k}{\mu}\tau_{KL}\frac{p_{KL}^n\rho_{KL}^n\psi_{KL}}{T_{KL}^n}\left(\frac{1}{\rho_L^n} - \frac{1}{\rho_K^n}\right)(p_L^n - p_K^n).\end{aligned}\tag{4.20}$$

Finally, combining (4.17) together with (4.18), (4.19) and (4.20), we conclude the proof. □

The following proposition provides a reformulation of the discrete entropy conservation equation (4.7), using the discrete entropy-energy relation (4.13)–(4.15) and the identity stated in Proposition 2.

**Proposition 3.** *Let $\psi_h \in H_h$ be a test function. The discrete entropy balance equation (4.7) is equivalent to*

$$\begin{aligned}&\sum_{K\in\mathcal{T}}|K|\left(S_{s,K}^n - S_{s,K}^{n-1} + \frac{\rho_K^{n-1}\phi_K^{n-1}}{T_K^n}\delta t\left(\partial_t^n e_K + p_K^n\partial_t^n\left(\frac{1}{\rho_K}\right)\right)\right)\psi_K\\&+ \frac{1}{2}\delta t\sum_{K\in\mathcal{T}}\sum_{L\in\mathcal{N}(K)}\frac{\rho_{KL}^n}{T_{KL}^n}\left(e_L^n - e_K^n\right)\frac{k}{\mu}\tau_{KL}\left(p_K^n - p_L^n\right)\frac{\psi_L + \psi_K}{2}\\&+ \frac{1}{2}\delta t\sum_{K\in\mathcal{T}}\sum_{L\in\mathcal{N}(K)}\frac{\rho_{KL}^n p_{KL}^n}{T_{KL}^n}\left(\frac{1}{\rho_L^n} - \frac{1}{\rho_K^n}\right)\frac{k}{\mu}\tau_{KL}\left(p_K^n - p_L^n\right)\frac{\psi_L + \psi_K}{2}\\&+ \delta t\sum_{K\in\mathcal{T}}\sum_{L\in\mathcal{N}(K)}\frac{\lambda}{T_{\mathrm{ref}}}(T_K^n - T_L^n)\psi_K\\&= \delta t\sum_{K\in\mathcal{T}}|K|\frac{h_{e,K}^n}{T_K^n}\psi_K - \delta t\sum_{K\in\mathcal{T}}|K|s_K^n h_{m,K}^n\psi_K.\end{aligned}\tag{4.21}$$

*Proof.* Let $\psi_h \in H_h$ be a test function. Multiplying equation (4.7) by $\psi_K$ and summing over $K$, we obtain

$$\begin{aligned}
&\sum_{K\in\mathcal{T}} |K| \left(S_{s,K}^n + \rho_K^n \phi_K^n s_K^n - S_{s,K}^{n-1} - \rho_K^{n-1}\phi_K^{n-1} s_K^{n-1}\right)\psi_K \\
&+ \delta t \sum_{K\in\mathcal{T}} \sum_{L\in\mathcal{N}(K)} \rho_{KL}^n s_{KL}^n \frac{k}{\mu}\tau_{KL}(p_K^n - p_L^n)\psi_K \\
&+ \delta t \sum_{K\in\mathcal{T}} \sum_{L\in\mathcal{N}(K)} \frac{\lambda}{T_{\mathrm{ref}}}\tau_{KL}\left(T_K^n - T_L^n\right)\psi_K = \delta t \sum_{K\in\mathcal{T}} |K| \frac{h_{e,K}^n}{T_K^n}\psi_K.
\end{aligned} \tag{4.22}$$

Substituting the discrete entropy-energy relation (4.13) in the first term of (4.22), we obtain

$$\begin{aligned}
&\sum_{K\in\mathcal{T}} |K| \left(\rho_K^n \phi_K^n s_K^n - \rho_K^{n-1}\phi_K^{n-1} s_K^{n-1}\right)\psi_K \\
&= \sum_{K\in\mathcal{T}} |K|\delta t \left(s_K^n \partial_t^n(\rho_K\phi_K) + \rho_K^{n-1}\phi_K^{n-1}\partial_t^n s_K\right)\psi_K \\
&= \sum_{K\in\mathcal{T}} |K|\delta t \left(s_K^n \partial_t^n(\rho_K\phi_K) + \frac{\rho_K^{n-1}\phi_K^{n-1}}{T_K^n}\left(\partial_t^n e_K + p_K^n \partial_t^n\left(\frac{1}{\rho_K}\right)\right)\right)\psi_K.
\end{aligned} \tag{4.23}$$

Moreover, we can rewrite the second term in (4.22) as follows:

$$\begin{aligned}
&\sum_{K\in\mathcal{T}} \sum_{L\in\mathcal{N}(K)} \rho_{KL}^n s_{KL}^n \frac{k}{\mu}\tau_{KL}\left(p_K^n - p_L^n\right)\psi_K \\
&= \sum_{K\in\mathcal{T}} \sum_{L\in\mathcal{N}(K)} \rho_{KL}^n (s_{KL}^n - s_K^n) \frac{k}{\mu}\tau_{KL}\left(p_K^n - p_L^n\right)\psi_K \\
&+ \sum_{K\in\mathcal{T}} \sum_{L\in\mathcal{N}(K)} \rho_{KL}^n s_K^n \frac{k}{\mu}\tau_{KL}\left(p_K^n - p_L^n\right)\psi_K \\
&= \frac{1}{2}\sum_{K\in\mathcal{T}} \sum_{L\in\mathcal{N}(K)} \rho_{KL}^n (s_L^n - s_K^n) \frac{k}{\mu}\tau_{KL}\left(p_K^n - p_L^n\right)\psi_K \\
&+ \sum_{K\in\mathcal{T}} \sum_{L\in\mathcal{N}(K)} \rho_{KL}^n s_K^n \frac{k}{\mu}\tau_{KL}\left(p_K^n - p_L^n\right)\psi_K.
\end{aligned} \tag{4.24}$$

Combining equations (4.23) and (4.24), equation (4.22) becomes

$$\begin{aligned}
&\sum_{K\in\mathcal{T}} |K| \left(S_{s,K}^n - S_{s,K}^{n-1}\right) \\
&+ \sum_{K\in\mathcal{T}} |K|\delta t \left(s_K^n \partial_t^n(\rho_K\phi_K) + \frac{\rho_K^{n-1}\phi_K^{n-1}}{T_K^n}\left(\partial_t^n e_K + p_K^n \partial_t^n\left(\frac{1}{\rho_K}\right)\right)\right)\psi_K \\
&+ \frac{\delta t}{2}\sum_{K\in\mathcal{T}} \sum_{L\in\mathcal{N}(K)} \rho_{KL}^n (s_L^n - s_K^n) \frac{k}{\mu}\tau_{KL}\left(p_K^n - p_L^n\right)\psi_K \\
&+ \delta t \sum_{K\in\mathcal{T}} \sum_{L\in\mathcal{N}(K)} \rho_{KL}^n s_K^n \frac{k}{\mu}\tau_{KL}\left(p_K^n - p_L^n\right)\psi_K \\
&+ \delta t \sum_{K\in\mathcal{T}} \sum_{L\in\mathcal{N}(K)} \frac{\lambda}{T_{\mathrm{ref}}}\tau_{KL}\left(T_K^n - T_L^n\right)\psi_K = \delta t \sum_{K\in\mathcal{T}} |K| \frac{h_{e,K}^n}{T_K^n}\psi_K.
\end{aligned} \tag{4.25}$$

Substituting the discrete mass conservation equation (4.5) in (4.25), we obtain

$$\begin{aligned}
&\sum_{K\in\mathcal{T}}|K|\left(S^n_{s,K}-S^{n-1}_{s,K}\right)+\sum_{K\in\mathcal{T}}|K|\delta t\left(\frac{\rho^{n-1}_K\phi^{n-1}_K}{T^n_K}\left(\partial^n_t e_K+p^n_K\partial^n_t\left(\frac{1}{\rho_K}\right)\right)\right)\psi_K\\
&+\frac{\delta t}{2}\sum_{K\in\mathcal{T}}\sum_{L\in\mathcal{N}(K)}\rho^n_{KL}(s^n_L-s^n_K)\frac{k}{\mu}\tau_{KL}\left(p^n_K-p^n_L\right)\psi_K\\
&+\delta t\sum_{K\in\mathcal{T}}\sum_{L\in\mathcal{N}(K)}\frac{\lambda}{T_{\text{ref}}}\tau_{KL}\left(T^n_K-T^n_L\right)\psi_K=\delta t\sum_{K\in\mathcal{T}}|K|\left(\frac{h^n_{e,K}}{T^n_K}-s^n_K h^n_{m,K}\right)\psi_K.
\end{aligned}\tag{4.26}$$

Finally, by applying Proposition 2 for the third term of equation (4.26), we obtain equation (4.21) which is the desired result. □

## 4.3 Discrete variational formulation

In this section, we show that the finite volume scheme (4.5)–(4.11) is equivalent to a discrete variational formulation. This is formulated in the following proposition.

**Proposition 4.** *Given $(h^0_{m,h},h^0_{e,h},\boldsymbol{h}^0_h)\in L^{2+d}_h$ and $(p^0_h,T^0_h,\boldsymbol{u}^0_h)\in L^{2+d}_h$. Find $(p^n_h,T^n_h,\boldsymbol{u}^n_h)\in L^{2+d}_h$ such that for all $(\varphi_h,\psi_h,\boldsymbol{\omega}_h)\in H^{2+d}_h$, the finite volume scheme (4.5)- (4.21)- (4.11) is equivalent to the variational formulation:*

$$\int_\Omega\frac{\rho^n_h\phi^n_h-\rho^{n-1}_h\phi^{n-1}_h}{\delta t}\varphi_h\,\mathrm{d}x+\frac{1}{d}\int_\Omega\rho^n_h\frac{k}{\mu}\boldsymbol{\nabla}_h p^n_h\cdot\boldsymbol{\nabla}_h\varphi_h\,\mathrm{d}x=\int_\Omega h^n_{m,h}\varphi_h\,\mathrm{d}x.\tag{4.27}$$

$$\begin{aligned}
&\int_\Omega\frac{S^n_{s,h}-S^{n-1}_{s,h}}{\delta t}\psi_h\,\mathrm{d}x+\int_\Omega\frac{\rho^{n-1}_h\phi^{n-1}_h}{T^n_h}\left(\partial^n_t e_h+p^n_h\partial^n_t\left(\frac{1}{\rho_h}\right)\right)\psi_h\,\mathrm{d}x\\
&-\frac{1}{d}\int_\Omega\frac{\rho^n_h k}{T^n_h\mu}\boldsymbol{\nabla}_h p^n_h\cdot\boldsymbol{\nabla}_h e^n_h\psi_h\,\mathrm{d}x-\frac{1}{d}\int_\Omega\frac{\rho^n_h p^n_h}{T^n_h}\frac{k}{\mu}\boldsymbol{\nabla}_h\left(\frac{1}{\rho^n_h}\right)\cdot\boldsymbol{\nabla}_h p^n_h\psi_h\,\mathrm{d}x\\
&+\frac{1}{d}\int_\Omega\frac{\lambda}{T_{\text{ref}}}\boldsymbol{\nabla}_h T^n_h\cdot\boldsymbol{\nabla}_h\psi_h\,\mathrm{d}x=\int_\Omega\left(\frac{h^n_{e,h}}{T^n_h}+s^n_h h^n_{m,h}\right)\psi_h\,\mathrm{d}x
\end{aligned}\tag{4.28}$$

$$\begin{aligned}
&\int_\Omega\partial^n_{tt}\boldsymbol{u}_h\cdot\boldsymbol{\omega}_h\,\mathrm{d}x+\frac{1}{d}\int_\Omega\frac{\mathcal{E}}{(1+\nu)}\epsilon(\boldsymbol{u}^n_h):\epsilon(\boldsymbol{\omega}_h)\,\mathrm{d}x\\
&+\int_\Omega\frac{\mathcal{E}\nu}{(1+\nu)(1-2\nu)}\mathrm{div}_h\boldsymbol{u}^n_h\mathbb{I}_d:\epsilon(\boldsymbol{\omega}_h)\,\mathrm{d}x\\
&-\int_\Omega(bp^n_h+3\alpha_s K_s(T^n_h-T_{\text{ref}}))\,\mathrm{div}_h(\boldsymbol{\omega}_h)\,\mathrm{d}x=\int_\Omega\boldsymbol{h}^n_h\cdot\boldsymbol{\omega}_h\,\mathrm{d}x.
\end{aligned}\tag{4.29}$$

*Proof.* Let $\varphi_h\in H_h$ be a test function. Multiplying the discrete mass conservation equation (4.5) by $\varphi_K$ and summing over all cells $K$, we obtain

$$\begin{aligned}
&\sum_{K\in\mathcal{T}}|K|\left(\rho(p^n_K)\phi(\boldsymbol{\mathcal{U}}^n_K)-\rho(p^{n-1}_K)\phi(\boldsymbol{\mathcal{U}}^{n-1}_K)\right)\varphi_K\\
&+\delta t\sum_{K\in\mathcal{T}}\sum_{L\in\mathcal{N}(K)}\rho^n_{KL}\frac{k}{\mu}\tau_{KL}\left(p^n_K-p^n_L\right)\varphi_K=\delta t\sum_{K\in\mathcal{T}}|K|h^n_{m,K}\varphi_K.
\end{aligned}$$

From the definition of the discrete functions, we have

$$\begin{aligned}
&\sum_{K\in\mathcal{T}}|K|\frac{\rho^n_K\phi^n_K-\rho^{n-1}_K\phi^{n-1}_K}{\delta t}\varphi_K=\int_\Omega\frac{\rho^n_h\phi^n_h-\rho^{n-1}_h\phi^{n-1}_h}{\delta t}\varphi_h\,\mathrm{d}x,\\
&\sum_{K\in\mathcal{T}}|K|h^n_{m,K}\varphi_K=\int_\Omega h^n_{m,h}\varphi_h\,\mathrm{d}x.
\end{aligned}$$

In addition, applying the discrete integrating by parts Lemma 2 together with the definition of the discrete gradient (4.1), we obtain

$$\begin{aligned}
&\sum_{K\in\mathcal{T}}\sum_{L\in\mathcal{N}(K)} \rho_{KL}^n \frac{k}{\mu}\tau_{KL}\left(p_K^n - p_L^n\right)\varphi_K \\
&= \sum_{\sigma_{KL}\in\mathcal{E}_h} d\rho_{KL}^n \frac{\mathbb{K}}{\mu}|\mathcal{D}_{KL}| \frac{p_L^n - p_K^n}{d_{KL}}\frac{\varphi_L^n - \varphi_K^n}{d_{KL}} \\
&= \sum_{\sigma_{KL}\in\mathcal{E}_h} d\rho_{KL}^n \frac{k}{\mu}|\mathcal{D}_{KL}| \left(\frac{p_L^n - p_K^n}{d_{KL}}\boldsymbol{n}_{KL}\right)\cdot\left(\frac{\varphi_L^n - \varphi_K^n}{d_{KL}}\right)\boldsymbol{n}_{KL} \\
&= \frac{1}{d}\sum_{\sigma_{KL}\in\mathcal{E}_h} \rho_{KL}^n \frac{k}{\mu}|\mathcal{D}_{KL}|\boldsymbol{\nabla}_h p^n_{h|\mathcal{D}_{KL}}\cdot\boldsymbol{\nabla}_h\varphi_{h|\mathcal{D}_{KL}} \\
&= \frac{1}{d}\int_\Omega \rho_h^n\frac{k}{\mu}\boldsymbol{\nabla}_h p_h^n\cdot\boldsymbol{\nabla}_h\varphi_h\,\mathrm{d}x
\end{aligned}$$

which establishes (4.27). To derive the variational formulation (4.28) on entropy, we use the reformulated discrete entropy conservation equation (4.21). From the definition of the discrete functions, we have

$$\begin{aligned}
&\sum_{K\in\mathcal{T}}|K|\left(\frac{S_{s,K}^n - S_{s,K}^{n-1}}{\delta t} + \frac{\rho_K^{n-1}\phi_K^{n-1}}{T_K^n}\delta t\left(\partial_t^n e_K + p_K^n\partial_t^n\left(\frac{1}{\rho_K}\right)\right)\right)\psi_K \\
&= \int_\Omega \frac{S_{s,h}^n - S_{s,h}^{n-1}}{\delta t}\psi_h + \frac{\rho_h^{n-1}\phi_h^{n-1}}{T_h^n}\delta t\left(\frac{e_h^n - e_h^{n-1}}{\delta t} + \frac{p_h^n}{\delta t}\left(\frac{1}{\rho_h^n} - \frac{1}{\rho_h^{n-1}}\right)\right)\psi_h\,\mathrm{d}x,
\end{aligned}$$

and

$$\sum_{K\in\mathcal{T}}|K|\left(\frac{h_{e,K}^n}{T_K^n} - s_K^n h_{m,K}^n\right)\psi_K = \int_\Omega\left(\frac{h_{e,h}^n}{T_h^n} - s_h^n h_{m,h}^n\right)\psi_h\,\mathrm{d}x.$$

Additionally, transforming the sum over cells to the sum over edges and using the definition of the discrete gradient, from the second term of (4.21) we obtain

$$\begin{aligned}
&\frac{1}{2}\sum_{K\in\mathcal{T}}\sum_{L\in\mathcal{N}(K)}\frac{\rho_{KL}^n}{T_{KL}^n}\left(e_L^n - e_K^n\right)\frac{k}{\mu}\tau_{KL}\left(p_K^n - p_L^n\right)\psi_{KL} \\
&= -\frac{1}{d}\int_\Omega\frac{\rho_h^n}{T_h^n}\frac{k}{\mu}\boldsymbol{\nabla}_h e_h^n\cdot\boldsymbol{\nabla}_h p_h^n\psi_h\,\mathrm{d}x.
\end{aligned}$$

In the same way, from the third term of (4.21) we get

$$\begin{aligned}
&\sum_{K\in\mathcal{T}}\sum_{L\in\mathcal{N}(K)}\frac{\rho_{KL}^n p_{KL}^n}{T_{KL}^n}\left(\frac{1}{\rho_L^n} - \frac{1}{\rho_K^n}\right)\frac{k}{\mu}\tau_{KL}\left(p_K^n - p_L^n\right)\psi_K \\
&= -\frac{1}{d}\int_\Omega\frac{\rho_h^n p_h^n}{T_h^n}\frac{k}{\mu}\boldsymbol{\nabla}_h\left(\frac{1}{\rho_h^n}\right)\cdot\boldsymbol{\nabla}_h p_h^n\psi_h\,\mathrm{d}x.
\end{aligned}$$

Furthermore, using the discrete integration by parts lemma and the definition of the discrete gradient, we get

$$\sum_{K\in\mathcal{T}}\sum_{L\in\mathcal{N}(K)}\frac{\lambda}{T_{\mathrm{ref}}}\tau_{KL}(T_K^n - T_L^n)\psi_K = \frac{1}{d}\int_\Omega\frac{\lambda}{T_{\mathrm{ref}}}\boldsymbol{\nabla}_h T_h^n\cdot\boldsymbol{\nabla}_h\psi_h\,\mathrm{d}x.$$

Finally, let $\boldsymbol{\omega}_h \in H_h^d$ be a test function. To derive the variational formulation (4.29) on the displacement, we multiply equation (4.11) by $\boldsymbol{\omega}_K$ then we sum over $K$ to obtain

$$\begin{aligned}
&\sum_{K\in\mathcal{T}} |K| \frac{\boldsymbol{u}_K^n + \boldsymbol{u}_K^{n-2} - 2\boldsymbol{u}_K^{n-1}}{\delta t} \cdot \boldsymbol{\omega}_K \\
&+ \delta t \sum_{K\in\mathcal{T}} \sum_{L\in\mathcal{N}(K)} \frac{\mathcal{E}}{(1+\nu)} \frac{\tau_{KL}}{2} \times \\
&\left[ ((\boldsymbol{u}_K - \boldsymbol{u}_L) \otimes \boldsymbol{n}_{KL}) \boldsymbol{n}_{KL} + [(\boldsymbol{u}_K - \boldsymbol{u}_L) \otimes \boldsymbol{n}_{KL}]^\top \boldsymbol{n}_{KL} \right] \cdot \boldsymbol{\omega}_K \\
&- \delta t \sum_{K\in\mathcal{T}} \sum_{L\in\mathcal{N}(K)} \frac{\mathcal{E}\nu}{(1+\nu)(1-2\nu)} |\sigma_{KL}| \left(\mathrm{div} \boldsymbol{u}^n \mathbb{I}_d\right)_{KL} \boldsymbol{n}_{KL} \cdot \boldsymbol{\omega}_K \\
&+ \delta t \sum_{K\in\mathcal{T}} \sum_{L\in\mathcal{N}(K)} |\sigma_{KL}| \left(b p_{KL}^n \mathbb{I}_d + 3\alpha_s K_s \left(T_{KL}^n - T_{\mathrm{ref}}\right) \mathbb{I}_d\right) \boldsymbol{n}_{KL} \cdot \boldsymbol{\omega}_K \\
&= \delta t \sum_{K\in\mathcal{T}} |K| \boldsymbol{h}_K^n \cdot \boldsymbol{\omega}_K.
\end{aligned} \tag{4.30}$$

From the definition of the discrete functions, we have

$$\begin{aligned}
\sum_{K\in\mathcal{T}} |K| \frac{\boldsymbol{u}_K^n + \boldsymbol{u}_K^{n-2} - 2\boldsymbol{u}_K^{n-1}}{\delta t^2} \cdot \boldsymbol{\omega}_K &= \int_\Omega \delta_{tt}^n \boldsymbol{u}_h \cdot \boldsymbol{\omega}_h \,\mathrm{d}x, \\
\sum_{K\in\mathcal{T}} |K| \boldsymbol{h}_K^n \cdot \boldsymbol{\omega}_K &= \int_\Omega \boldsymbol{h}_h^n \cdot \boldsymbol{\omega}_h \,\mathrm{d}x.
\end{aligned}$$

By applying the discrete integration by parts Lemma 2 together with the definition of the contracted product, from the second term of (4.30) we obtain

$$\begin{aligned}
&\frac{1}{2} \sum_{K\in\mathcal{T}} \sum_{L\in\mathcal{N}(K)} \frac{\mathcal{E}}{(1+\nu)} \tau_{KL} \times \\
&\left( ([\boldsymbol{u}_K^n - \boldsymbol{u}_L^n] \otimes \boldsymbol{n}_{KL}) \boldsymbol{n}_{KL} + ([\boldsymbol{u}_K^n - \boldsymbol{u}_L^n] \otimes \boldsymbol{n}_{KL})^\top \boldsymbol{n}_{KL} \right) \cdot \boldsymbol{\omega}_K \\
&= d \sum_{\sigma_{KL}\in\mathcal{D}_{KL}} \frac{\mathcal{E}}{(1+\nu)} |\mathcal{D}_{KL}| \times \\
&\left[ \frac{1}{2d_{KL}} ([\boldsymbol{u}_L^n - \boldsymbol{u}_K^n] \otimes \boldsymbol{n}_{KL}) \boldsymbol{n}_{KL} + \frac{1}{2d_{KL}} ([\boldsymbol{u}_L^n - \boldsymbol{u}_K^n] \otimes \boldsymbol{n}_{KL})^\top \boldsymbol{n}_{KL} \right] \cdot \frac{\boldsymbol{\omega}_L - \boldsymbol{\omega}_K}{d_{KL}} \\
&= d \sum_{\sigma_{KL}\in\mathcal{D}_{KL}} \frac{\mathcal{E}}{(1+\nu)} \frac{|\mathcal{D}_{KL}|}{2d_{KL}} \times \\
&\sum_{i,j=1}^{d} \left[ \left(u_{i,L}^n - u_{i,K}^n\right) n_{j,KL} + \left(u_{j,L}^n - u_{j,K}^n\right) n_{i,KL} \right] \frac{\omega_{i,L} - \omega_{i,K}}{d_{KL}} n_{j,KL}.
\end{aligned} \tag{4.31}$$

In addition, employing the identity $2\sum_{i,j} a_i b_j = \sum_{i,j} a_i b_j + \sum_{i,j} a_j b_i$ for all $a_i, b_j \in \mathbb{R}$ on the right-hand side of (4.31). For the first term, we take $a_i = (u_{i,L}^n - u_{i,K}^n)(\omega_{i,L} - \omega_{i,K})$ and $b_j = n_{j,KL} n_{j,KL}$; for the second term, we set $a_i = (\omega_{i,L} - \omega_{i,K}) n_{i,KL}$ and $b_j = (u_{j,L}^n - u_{j,K}^n) n_{j,KL}$. Together with the definition of the double contracted product and the stress tensor, this yields

$$\frac{1}{2}\sum_{K\in\mathcal{T}}\sum_{L\in\mathcal{N}(K)}\frac{\mathcal{E}}{(1+\nu)}\tau_{KL}\times$$
$$\Big(([\boldsymbol{u}_K^n-\boldsymbol{u}_L^n]\otimes\boldsymbol{n}_{KL})\,\boldsymbol{n}_{KL}+([\boldsymbol{u}_K^n-\boldsymbol{u}_L^n]\otimes\boldsymbol{n}_{KL})^\top\,\boldsymbol{n}_{KL}\Big)\cdot\boldsymbol{\omega}_K$$
$$=\frac{1}{d}\sum_{\sigma_{KL}\in\mathcal{D}_{KL}}\frac{\mathcal{E}}{(1+\nu)}\frac{|\mathcal{D}_{KL}|}{4d_{KL}^2}\times$$
$$\sum_{i,j=1}^{d}\Big[(\boldsymbol{\nabla}_h\boldsymbol{u}_h^n\otimes\boldsymbol{n}_{KL})_{i,j}+(\boldsymbol{\nabla}_h\boldsymbol{u}_h^n\otimes\boldsymbol{n}_{KL})_{j,i}\Big]_{|\mathcal{D}_{KL}}\Big[(\boldsymbol{\nabla}_h\boldsymbol{\omega}_h\otimes\boldsymbol{n}_{KL})_{i,j}+(\boldsymbol{\nabla}_h\boldsymbol{\omega}_h\otimes\boldsymbol{n}_{KL})_{j,i}\Big]_{|\mathcal{D}_{KL}}$$
$$=\frac{1}{d}\sum_{\sigma_{KL}\in\mathcal{D}_{KL}}\frac{\mathcal{E}}{(1+\nu)}|\mathcal{D}_{KL}|\sum_{i,j=1}^{d}\epsilon(\boldsymbol{u}_h^n)_{i,j|\mathcal{D}_{KL}}\epsilon(\boldsymbol{\omega}_h)_{i,j|\mathcal{D}_{KL}}=\frac{1}{d}\int_\Omega\frac{\mathcal{E}}{(1+\nu)}\epsilon(\boldsymbol{u}_h^n):\epsilon(\boldsymbol{\omega}_h)\,\mathrm{d}x.$$

Proceeding analogously, we treat the third term of (4.30) to obtain

$$-\sum_{K\in\mathcal{T}}\sum_{L\in\mathcal{N}(K)}\frac{\mathcal{E}\nu}{(1+\nu)(1-2\nu)}|\sigma_{KL}|(\mathrm{div}\boldsymbol{u}^n)_{KL}\mathbb{I}_d\boldsymbol{n}_{KL}\cdot\boldsymbol{\omega}_K$$
$$=\int_\Omega\frac{\mathcal{E}\nu}{(1+\nu)(1-2\nu)}\mathrm{div}_h\boldsymbol{u}_h^n\mathbb{I}_d:\epsilon(\boldsymbol{\omega}_h)\,\mathrm{d}x.$$

Finally, for the fourth term of (4.30), we first consider the pressure term. Integrating by parts and applying the definition of the discrete divergence operator (4.3) together with the boundary conditions, we obtain

$$\sum_{K\in\mathcal{T}}\sum_{L\in\mathcal{N}(K)}b|\sigma_{KL}|p_{KL}^n\mathbb{I}_d\boldsymbol{n}_{KL}\cdot\boldsymbol{\omega}_K$$
$$=-\frac{1}{2}\sum_{K\in\mathcal{T}}\sum_{L\in\mathcal{N}(K)}|\sigma_{KL}|b\,[p_{KL}^n(\boldsymbol{\omega}_L-\boldsymbol{\omega}_K)]\cdot\boldsymbol{n}_{KL}$$
$$=-\frac{1}{4}\sum_{K\in\mathcal{T}}\sum_{L\in\mathcal{N}(K)}|\sigma_{KL}|b\,[2(p_L^n\boldsymbol{\omega}_L-p_K^n\boldsymbol{\omega}_K)-(\boldsymbol{\omega}_K+\boldsymbol{\omega}_L)(p_L^n-p_K^n)]\cdot\boldsymbol{n}_{KL}$$
$$=-\frac{1}{4}\sum_{K\in\mathcal{T}}\sum_{L\in\mathcal{N}(K)}|\sigma_{KL}|b\,[2(p_L^n\boldsymbol{\omega}_L-p_K^n\boldsymbol{\omega}_K)\cdot\boldsymbol{n}_{KL}+2p_K^n(\boldsymbol{\omega}_K+\boldsymbol{\omega}_L)\cdot\boldsymbol{n}_{KL}]$$
$$=-\sum_{K\in\mathcal{T}}|K|bp_K^n\mathrm{div}_K\boldsymbol{\omega}_h.$$

Similarly, we obtain

$$\sum_{K\in\mathcal{T}}\sum_{L\in\mathcal{N}(K)}|\sigma_{KL}|(3\alpha_sK_s(T_{KL}^n-T_{\mathrm{ref}}))\boldsymbol{n}_{KL}\cdot\boldsymbol{\omega}_K$$
$$=-\sum_{K\in\mathcal{T}}|K|3\alpha_sK_s(T_K^n-T_{\mathrm{ref}})\mathrm{div}_K\boldsymbol{\omega}_h.$$

Therefore, we obtain

$$\sum_{K\in\mathcal{T}}\sum_{L\in\mathcal{N}(K)}[b|\sigma_{KL}|p_{KL}^n+|\sigma_{KL}|3\alpha_sK_s(T_{KL}^n-T_{\mathrm{ref}})]\,\boldsymbol{n}_{KL}\cdot\boldsymbol{\omega}_K$$
$$=-\int_\Omega(bp_h^n+3\alpha_sK_s(T_h^n-T_{\mathrm{ref}}))\mathrm{div}_h\boldsymbol{\omega}_h\,\mathrm{d}x,$$

which establishes the desired result. □

## 5 Discrete energy estimates

In this section, we derive the discrete energy estimates for the model under Assumption 1 on the discrete physical data. The following lemma provides a key estimate that will be used to derive the discrete energy estimates.

**Lemma 3.** *Let $(\boldsymbol{u}_h^n, p_h^n, T_h^n)$ be the solution to the system of equations (4.27)–(4.29). Then, the following estimate holds*

$$\begin{aligned}
&\int_\Omega \partial_t^n E_h \,\mathrm{d}x + \int_\Omega \frac{m_0}{2}\partial_t^n|\partial_t^n \boldsymbol{u}_h|^2 \,\mathrm{d}x - \int_\Omega \phi_h^{n-1}\frac{\tilde{\rho}_h'}{\rho_h^n} p_h^n \partial_t^n p_h \,\mathrm{d}x \\
&+ \frac{k}{d\,\mu}\|\boldsymbol{\nabla}_h p_h^n\|^2_{L^2(\Omega)} + \frac{\lambda}{d\,T_{\mathrm{ref}}}\|\boldsymbol{\nabla}_h T_h^n\|^2_{L^2(\Omega)} + \frac{1}{d}\int_\Omega \frac{k\overline{\rho}_h'}{\mu \rho_h^n} p_h^n \,|\boldsymbol{\nabla}_h p_h^n|^2 \,\mathrm{d}x \\
&\leq \int_\Omega \left(h_{m,h}^n(g_h^n + e_h^n - s_h^n T_h^n) + h_{e,h}^n + \boldsymbol{h}_h^n \cdot \partial_t^n \boldsymbol{u}_h\right) \mathrm{d}x.
\end{aligned} \tag{5.1}$$

*Where the discrete energy $E_h^n$ is defined by*

$$\begin{aligned}
E_h^n :=& \rho_h^n \phi_h^n g_h^n - \phi_h^n p_h^n + \rho_h^n \phi_h^n e_h^n + \frac{1}{2}\begin{bmatrix} p_h^n & T_h^n \end{bmatrix} \mathbb{M} \begin{bmatrix} p_h^n \\ T_h^n \end{bmatrix} \\
&+ \frac{\mathcal{E}}{2d(1+\nu)}|\epsilon(\boldsymbol{u}_h^n)|^2 + \frac{\mathcal{E}\nu}{2(1+\nu)(1-2\nu)}(\mathrm{div}_h \boldsymbol{u}_h^n)^2,
\end{aligned}$$

*with $\tilde{\rho}_h = \rho(c_h)$ with $c_h \in ]p_h^{n-1}, p_h^n[$, $\overline{\rho}_h = \rho(z_h^n)$ with $z_h^n \in ]p_K^n, p_L^n[$, the matrix $\mathbb{M}$ is defined by (3.4) and the function $g$ is defined by (3.1).*

*Proof.* First, we consider in (4.27)–(4.29), the test functions $\varphi_h = (g(p_h^n) + e_h^n) \in H_h$ where $g$ is defined by $g(p_h^n) := \displaystyle\int_0^{p_h^n} \frac{1}{\rho(\zeta)}\, d\zeta$, $\psi_h = T_h^n \in H_h$ and $\boldsymbol{\omega}_h = \partial_t^n \boldsymbol{u}_h \in H_h^d$. Then, summing the resulting equations, we obtain

$$E_1 + E_2 + E_3 + E_4 + E_5 + E_6 = E_7, \tag{5.2}$$

where

$$\begin{aligned}
E_1 &= \int_\Omega \frac{\rho_h^n \phi_h^n - \rho_h^{n-1}\phi_h^{n-1}}{\delta t}(g(p_h^n) + e_h^n)\,\mathrm{d}x \\
&\quad + \int_\Omega \rho_h^{n-1}\phi_h^{n-1}\left(\partial_t^n e_h + p_h^n \partial_t^n \left(\frac{1}{\rho_h}\right)\right) \mathrm{d}x, \\
E_2 &= \int_\Omega \frac{S_{s,h}^n - S_{s,h}^{n-1}}{\delta t} T_h^n \,\mathrm{d}x, \\
E_3 &= \frac{1}{d}\int_\Omega \rho_h^n \frac{k}{\mu}\boldsymbol{\nabla}_h p_h^n \cdot \boldsymbol{\nabla}_h g(p_h^n)\,\mathrm{d}x + \frac{1}{d}\int_\Omega -\rho_h^n p_h^n \frac{k}{\mu}\boldsymbol{\nabla}_h\left(\frac{1}{\rho_h^n}\right)\cdot \boldsymbol{\nabla}_h p_h^n \,\mathrm{d}x, \\
E_4 &= \frac{\lambda}{d\,T_{\mathrm{ref}}}\|\boldsymbol{\nabla}_h T_h^n\|^2_{L^2(\Omega)}, \\
E_5 &= \int_\Omega \partial_{tt}^n \boldsymbol{u}_h \cdot \partial_t^n \boldsymbol{u}_h \,\mathrm{d}x + \frac{1}{d}\int_\Omega \frac{\mathcal{E}}{(1+\nu)}\epsilon(\boldsymbol{u}_h^n) : \epsilon(\partial_t \boldsymbol{u}_h^n)\,\mathrm{d}x \\
&\quad + \int_\Omega \frac{\mathcal{E}\nu}{(1+\nu)(1-2\nu)}\mathrm{div}_h \boldsymbol{u}_h^n \mathbb{I}_d : \epsilon(\partial_t \boldsymbol{u}_h^n)\,\mathrm{d}x, \\
E_6 &= -\int_\Omega (b p_h^n + 3\alpha_s K_s (T_h^n - T_{\mathrm{ref}}))\,\mathrm{div}_h(\partial_t \boldsymbol{u}_h^n)\,\mathrm{d}x, \\
E_7 &= \int_\Omega \left(h_{m,h}^n(g(p_h^n) + e_h^n - s_h^n T_h^n) + h_{e,h}^n + \boldsymbol{h}_h^n \cdot \partial_t \boldsymbol{u}_h^n\right) \mathrm{d}x.
\end{aligned}$$

Expanding $E_1$, we obtain

$$E_1 = \int_\Omega \partial_t^n(\rho_h\phi_h e_h + \rho_h\phi_h g(p_h))\,\mathrm{d}x + \frac{1}{\delta t}\int_\Omega \rho_h^{n-1}\phi_h^{n-1}(g(p_h^{n-1}) - g(p_h^n))\,\mathrm{d}x$$
$$+ \int_\Omega \rho_h^{n-1}\phi_h^{n-1}p_h^n\partial_t^n\left(\frac{1}{\rho_h}\right)\,\mathrm{d}x := E_{1,1} + E_{1,2} + E_{1,3}.$$

Since the function $g$ is concave ($g'' \leq 0$), then we have

$$g(p_h^n) - g(p_h^{n-1}) \leq g'(p_h^{n-1})(p_h^n - p_h^{n-1}).$$

Consequently, $E_{1,2}$ can be bounded as follows

$$E_{1,2} \geq \frac{1}{\delta t}\int_\Omega \left[p_h^n(\phi_h^n - \phi_h^{n-1}) - \delta t\partial_t^n(\phi_h p_h)\right]\,\mathrm{d}x.$$

Next, from the mean value theorem [23], we have

$$\rho_h^n - \rho_h^{n-1} = (\tilde{\rho}_h)'(p_h^n - p_h^{n-1}),$$

where $\tilde{\rho}_h = \rho(c_h)$ with $c_h \in ]p_h^{n-1}, p_h^n[$. Consequently, from $E_{1,3}$, we obtain

$$\rho_h^{n-1}\phi_h^{n-1}p_h^n\partial_t^n\left(\frac{1}{\rho_h}\right) = -\phi_h^{n-1}\frac{(\tilde{\rho}_h)'}{\rho_h^n}p_h^n\partial_t^n p_h.$$

We thus obtain the following lower bound for $E_1$:

$$\begin{aligned} E_1 \geq &\int_\Omega \partial_t^n\left(\rho_h\phi_h e_h + \rho_h\phi_h g(p_h) - \phi_h p_h\right)\,\mathrm{d}x \\ &+ \frac{1}{\delta t}\int_\Omega p_h^n(\phi_h^n - \phi_h^{n-1})\,\mathrm{d}x - \int_\Omega \phi_h^{n-1}\frac{(\tilde{\rho}_h)'}{\rho_h^n}p_h^n\partial_t^n p_h\,\mathrm{d}x. \end{aligned} \tag{5.3}$$

Furthermore, from the definition of the discrete porosity and skeleton entropy (4.12), we obtain

$$\begin{aligned} &\int_\Omega p_h^n\frac{\phi_h^n - \phi_h^{n-1}}{\delta t}\,\mathrm{d}x + \int_\Omega T_h^n\frac{S_{s,h}^n - S_{s,h}^{n-1}}{\delta t}\,\mathrm{d}x - \int_\Omega (bp_h^n + 3\alpha_s K_s(T_h^n))\,\mathrm{div}_h\partial_t^n(\boldsymbol{u}_h)\,\mathrm{d}x \\ &= \int_\Omega \left(-3\alpha_\phi p_h^n\frac{T_h^n - T_h^{n-1}}{\delta t} + \frac{1}{N}p_h^n\frac{p_h^n - p_h^{n-1}}{\delta t} - 3\alpha_\phi T_h^n\frac{p_h^n - p_h^{n-1}}{\delta t} + \frac{C_s}{T_{\text{ref}}}T_h^n\frac{T_h^n - T_h^{n-1}}{\delta t}\right)\,\mathrm{d}x \\ &= \int_\Omega \frac{1}{\delta t}\left[\begin{bmatrix} p_h^n & T_h^n \end{bmatrix}\mathbb{M}\begin{bmatrix} p_h^n - p_h^{n-1} \\ T_h^n - T_h^{n-1} \end{bmatrix}\right]\,\mathrm{d}x. \end{aligned}$$

Moreover, since $\mathbb{M}$ is a real, symmetric, positive definite matrix, we have the following inequality

$$\begin{aligned} \frac{1}{\delta t}\left[\begin{bmatrix} p_h^n & T_h^n \end{bmatrix}\mathbb{M}\begin{bmatrix} p_h^n - p_h^{n-1} \\ T_h^n - T_h^{n-1} \end{bmatrix}\right] &\geq \frac{1}{2\delta t}\left[\begin{bmatrix} p_h^n & T_h^n \end{bmatrix}\mathbb{M}\begin{bmatrix} p_h^n \\ T_h^n \end{bmatrix} - \begin{bmatrix} p_h^{n-1} & T_h^{n-1} \end{bmatrix}\mathbb{M}\begin{bmatrix} p_h^{n-1} \\ T_h^{n-1} \end{bmatrix}\right] \\ &= \frac{1}{2}\partial_t^n\left[\begin{bmatrix} p_h & T_h \end{bmatrix}\mathbb{M}\begin{bmatrix} p_h \\ T_h \end{bmatrix}\right]. \end{aligned}$$

This yields

$$E_{1,2} + E_2 + E_6 \geq -\int_\Omega \partial_t^n(\phi_h p_h)\,\mathrm{d}x + \frac{1}{2}\int_\Omega \partial_t^n\left[\begin{bmatrix} p_h & T_h \end{bmatrix}\mathbb{M}\begin{bmatrix} p_h \\ T_h \end{bmatrix}\right]\,\mathrm{d}x. \tag{5.4}$$

Furthermore, we recall the inequality $a(a-b) \geq \frac{1}{2}(a^2 - b^2)$ for all $a, b \in \mathbb{R}$, which yields the bound

$$\partial_{tt}^n\boldsymbol{u}_h \cdot \partial_t^n\boldsymbol{u}_h = \frac{1}{\delta t}\left(\partial_t^n\boldsymbol{u}_h - \partial_t^{n-1}\boldsymbol{u}_h\right)\cdot\partial_t^n\boldsymbol{u}_h \geq \frac{1}{2}\partial_t^n|\partial_t^n\boldsymbol{u}_h|^2. \tag{5.5}$$

In the same way, the second term of $E_5$ satisfies

$$\epsilon(\boldsymbol{u}_h^n) : \epsilon(\partial_t^n \boldsymbol{u}_h) = \frac{1}{\delta t}\epsilon(\boldsymbol{u}_h^n) : \epsilon(\boldsymbol{u}_h^n - \boldsymbol{u}_h^{n-1}) \geq \frac{1}{2}\partial_t^n(|\epsilon(\boldsymbol{u}_h)|^2), \tag{5.6}$$

Likewise, the third term of $E_5$ satisfies

$$\mathrm{div}_h \boldsymbol{u}_h^n \mathbb{I}_d : \epsilon(\partial_t^n \boldsymbol{u}_h) = \frac{1}{\delta t}\left(\mathrm{div}_h \boldsymbol{u}_h^n \mathbb{I}_d : \epsilon(\boldsymbol{u}_h^n - \boldsymbol{u}_h^{n-1})\right) \geq \frac{1}{2}\partial_t^n(\mathrm{div}_h \boldsymbol{u}_h)^2. \tag{5.7}$$

Combining the three estimates (5.5), (5.6) and (5.7) yields

$$E_5 \geq \frac{1}{2}\int_\Omega \left[\partial_t^n|\partial_t^n \boldsymbol{u}_h|^2 + \frac{\mathcal{E}}{d(1+\nu)}\partial_t^n(|\epsilon(\boldsymbol{u}_h)|^2) + \frac{\mathcal{E}\nu}{(1+\nu)(1-2\nu)}\partial_t^n(\mathrm{div}_h \boldsymbol{u}_h)^2\right] \mathrm{d}x. \tag{5.8}$$

Now, to obtain the estimate on the gradient terms, we note that

$$g(p_L^n) - g(p_K^n) = \int_{p_K^n}^{p_L^n} \frac{1}{\rho(\zeta)} d\zeta,$$

and from the definition of the density on the interfaces (4.6), we have

$$\rho_{KL}^n(g(p_L^n) - g(p_K^n)) = p_L^n - p_K^n.$$

Then, by considering $g_h^n = (g(p_K^n))_{K\in\mathcal{T}}$, we get

$$\rho_h^n \boldsymbol{\nabla}_h g^n_{h|\mathcal{D}_{KL}} = d\rho_{KL}\frac{g(p_L^n) - g(p_K^n)}{d_{KL}}\boldsymbol{n}_{KL} = d\frac{p_L^n - p_K^n}{d_{KL}}\boldsymbol{n}_{KL} = \boldsymbol{\nabla}_h p^n_{h|\mathcal{D}_{KL}},$$

and

$$\rho_h^n \boldsymbol{\nabla}_h p_h^n \cdot \boldsymbol{\nabla}_h g^n_{h|\mathcal{D}_{KL}} = (\boldsymbol{\nabla}_h p_h^n \cdot \boldsymbol{\nabla}_h p_h^n)_{|\mathcal{D}_{KL}}.$$

Finally, using the mean value theorem, from $E_3$, we have

$$\begin{aligned} -\rho_h^n p_h^n \boldsymbol{\nabla}_h\left(\frac{1}{\rho_h^n}\right)\cdot \boldsymbol{\nabla}_h p_h^n{}_{|\mathcal{D}_{KL}} &= -d^2\frac{\rho_{KL}^n p_{KL}^n}{d_{KL}}\left(\frac{1}{\rho_L^n} - \frac{1}{\rho_K^n}\right)\frac{p_L^n - p_K^n}{d_{KL}} \\ = d^2\overline{\rho}_h'\frac{\rho_{KL}^n p_{KL}^n}{\rho_L^n\rho_K^n}\left(\frac{p_L^n - p_K^n}{d_{KL}}\right)\frac{p_L^n - p_K^n}{d_{KL}} &= \overline{\rho}_h'\frac{\rho_{KL}^n p_{KL}^n}{\rho_L^n\rho_K^n}(\boldsymbol{\nabla}_h p_h^n \cdot \boldsymbol{\nabla}_h p_h^n)_{|\mathcal{D}_{KL}}, \end{aligned} \tag{5.9}$$

where $\overline{\rho}_h' = \rho'(z_h^n)$ with $z_h^n \in (p_K^n, p_L^n)$. In addition, since $g$ is concave, we have

$$g(p_K^n) - g(p_L^n) \leq g'(p_L^n)(p_K^n - p_L^n). \tag{5.10}$$

Using the definition of the density on the interface (4.6) and inequality (5.10), we obtain

$$\rho_{KL}^n = \frac{p_K^n - p_L^n}{g(p_K^n) - g(p_L^n)} \geq \frac{1}{g'(p_L^n)} = \rho(p_L^n).$$

Since $\rho_{KL}$ is symmetric, we also have $\rho_{KL}^n \geq \rho(p_K^n)$. Hence, from (5.9), we obtain

$$-\int_\Omega \rho_h^n p_h^n \frac{\mathbb{K}}{\mu}\boldsymbol{\nabla}_h\left(\frac{1}{\rho_h^n}\right)\cdot \boldsymbol{\nabla}_h p_h^n \,\mathrm{d}x \geq \int_\Omega \frac{\overline{\rho}_h'}{\rho_h^n} p_h^n \left|\boldsymbol{\nabla}_h p_h^n\right|^2 \mathrm{d}x.$$

This yields the following bound for $E_3$

$$E_3 \geq \frac{k}{d\mu}\|\boldsymbol{\nabla}_h p_h^n\|^2_{L^2(\Omega)} + \frac{1}{d}\int_\Omega \frac{k\overline{\rho}_h'}{\mu\rho_h^n} p_h^n \left|\boldsymbol{\nabla}_h p_h^n\right|^2 \mathrm{d}x. \tag{5.11}$$

To conclude, we combine the estimates obtained in (5.3), (5.4), (5.8) and (5.11) which completes the proof. □

We now state the main discrete energy estimate for our model in the form of the following proposition.

**Proposition 5.** *Let $(\boldsymbol{u}_h^n, p_h^n, T_h^n)$ be the solution of (4.27)–(4.29). We assume that Assumption 1 holds. We also assume that the discrete fluid pressure is positive, the porosity is constant ($\phi_h^n = \_0$) and $\phi_0\gamma$ is sufficiently small; we obtain the following estimate:*

$$\begin{aligned}&\|\partial_t \boldsymbol{u}_{\mathscr{D}}\|_{L^\infty(0,t_F,L^2(\Omega))} + \|p_{\mathscr{D}}\|_{L^\infty(0,t_F,L^2(\Omega))} + \|T_{\mathscr{D}}\|_{L^\infty(0,t_F,L^2(\Omega))} + \|e_{\mathscr{D}}\|_{L^\infty(0,t_F,L^1(\Omega))}\\ &+ \|\boldsymbol{u}_{\mathscr{D}}\|_{L^\infty(0,t_F,H^1(\Omega))} + \|\boldsymbol{\nabla}_h p_{\mathscr{D}}\|_{L^2(0,t_F,L^2(\Omega))} + \|\boldsymbol{\nabla}_h T_{\mathscr{D}}\|_{L^2(0,t_F,L^2(\Omega))} \leq C.\end{aligned} \tag{5.12}$$

*Proof.* From Lemma 3, we recall that the solution $(\boldsymbol{u}_h^n, p_h^n, T_h^n)$ satisfies the discrete estimate (5.1). Summing inequality (5.1) over $n = 1, ..., N_T$, we obtain

$$\begin{aligned}&\int_\Omega \left(E_h^{N_T} - E_h^0\right) \mathrm{d}x + \int_\Omega \frac{m_0}{2}\left(\left|\partial_t^{N_T}\boldsymbol{u}_h\right|^2 - \left|\partial_t^0\boldsymbol{u}_h\right|^2\right) \mathrm{d}x\\ &- \sum_{n=1}^{N_T}\int_\Omega \phi_h^{n-1}\frac{\tilde{\rho}_h'}{\rho_h^n} p_h^n(p_h^n - p_h^{n-1})\,\mathrm{d}x + \frac{\delta t}{d}\sum_{n=1}^{N_T}\int_\Omega \frac{k}{\mu}\left|\boldsymbol{\nabla}_h p_h^n\right|^2 \mathrm{d}x\\ &+ \frac{\delta t}{d}\sum_{n=1}^{N_T}\int_\Omega \frac{\lambda}{T_{\text{ref}}}\left|\boldsymbol{\nabla}_h T_h^n\right|^2 \mathrm{d}x + \frac{\delta t}{d}\sum_{n=1}^{N_T}\int_\Omega \frac{k\overline{\rho}_h'}{\mu\rho_h^n} p_h^n\left|\boldsymbol{\nabla}_h p_h^n\right|^2 \mathrm{d}x\\ &\leq \delta t\sum_{n=1}^{N_T}\int_\Omega \left(h_{m,h}^n\left(g(p_h^n) + e_h^n - s_h^n T_h^n\right) + h_{e,h}^n + \boldsymbol{h}_h^n\cdot\partial_t^n\boldsymbol{u}_h\right) \mathrm{d}x.\end{aligned} \tag{5.13}$$

Moreover, using Assumption 1 (**A6**), and the fact that $p_h^n \geq 0$ and the porosity is constant, we obtain the following inequalities from the third term of (5.13) depending on the monotonicity of the pressure:

**If $p_h^n - p_h^{n-1} \geq 0$:**

$$-\phi_h^{n-1}\frac{\tilde{\rho}_h'}{\rho_h^n} p_h^n(p_h^n - p_h^{n-1}) = -\phi_0\gamma((p_h^n)^2 - p_h^n p_h^{n-1}) \geq -\phi_0\gamma((p_h^n)^2 - (p_h^{n-1})^2).$$

**If $p_h^n - p_h^{n-1} < 0$:**

$$-\phi_h^{n-1}\frac{\tilde{\rho}_h'}{\rho_h^n} p_h^n(p_h^n - p_h^{n-1}) \geq 0 \geq \phi_0\gamma((p_h^n)^2 - (p_h^{n-1})^2).$$

Consequently, we obtain

$$-\phi_h^{n-1}\frac{\tilde{\rho}_h'}{\rho_h^n} p_h^n(p_h^n - p_h^{n-1}) \geq -\text{sgn}(p_h^n - p_h^{n-1})\phi_0\gamma((p_h^n)^2 - (p_h^{n-1})^2), \tag{5.14}$$

where $\text{sgn}(p_h^n - p_h^{n-1}) := \begin{cases} 1 & \text{if } p_h^n - p_h^{n-1} \geq 0,\\ -1 & \text{otherwise.}\end{cases}$

Let $\{y^{N_T}\}_{N_T=1}^\infty$ be the sequence defined by

$$y^{N_T} := \int_\Omega \left(E_h^{N_T} + \frac{m_0}{2}\left|\partial_t^{N_T}\boldsymbol{u}_h\right|^2 - \text{sgn}(p_h^n - p_h^{n-1})\phi_0\gamma\left(p_h^{N_T}\right)^2\right) \mathrm{d}x.$$

Our goal is to apply the discrete Gronwall Lemma [9]. To that end, we aim to show that there exist two sequences $\{a^{N_T}\}_{N_T=1}^\infty$ and $\{b^{N_T}\}_{N_T=1}^\infty$ such that $y^{N_T} \leq a^{N_T} + \sum_{n=1}^{N_T} y^n b^n$, which is the required form to apply the Gronwall Lemma and conclude the desired bound. Using the definition of $y^{N_T}$ and inequalities (5.13) and (5.14), we obtain:

$$\begin{aligned}y^{N_T} - y^0 &= \int_\Omega \left(E_h^{N_T} - E_h^0\right) \mathrm{d}x + \int_\Omega \frac{m_0}{2}\left(\left|\partial_t^{N_T}\boldsymbol{u}_h\right|^2 - \left|\partial_t^0\boldsymbol{u}_h\right|^2\right) \mathrm{d}x\\ &- \int_\Omega \text{sgn}(p_h^n - p_h^{n-1})\phi_0\gamma\left(\left(p_h^{N_T}\right)^2 - \left(p_h^0\right)^2\right) \mathrm{d}x\\ &\leq \delta t\sum_{n=1}^{N_T}\int_\Omega \left(h_{m,h}^n\left(g(p_h^n) + e_h^n - s_h^n T_h^n\right) + h_{e,h}^n + \boldsymbol{h}_h^n\cdot\partial_t^n\boldsymbol{u}_h\right) \mathrm{d}x.\end{aligned} \tag{5.15}$$

Applying the Cauchy-Schwarz inequality, we have

$$\int_\Omega \boldsymbol{h}_h^n \cdot \partial_t^n \boldsymbol{u}_h \mathrm{d}x \leq \|\boldsymbol{h}_h^n\|_{L^2(\Omega)} \|\partial_t^n \boldsymbol{u}_h\|_{L^2(\Omega)}. \tag{5.16}$$

From Assumptions **(A2)** and **(A3)**, there exist positive constants $C_1$, $C_2$, $C_3$ and $C_4 \in \mathbb{R}_+$ such that

$$|h_{m,h}^n| \leq C_1, \quad |h_{e,h}^n| \leq C_2, \quad |\boldsymbol{h}_h^n| \leq C_3 \quad \text{and} \quad e_h^n - T_h^n s_h^n \leq C_4(|p_h^n|^2 + |T_h^n|^2). \tag{5.17}$$

In addition, since the function $g$ is sublinear, it follows that there exists a constant $C_5 \in \mathbb{R}_+$ such that

$$g(p_h^n) \leq C_5 p_h^n. \tag{5.18}$$

Analogous to the continuous case, we employ inequality (5.16), the bounds (5.17) and (5.18), and we apply Young's inequality $\big(ab \leq \frac{1}{2}(a^2+b^2),\ \forall a, b \in \mathbb{R}\big)$ to obtain

$$\begin{aligned} &\int_\Omega \left(h_{m,h}^n \left(g(p_h^n) + e_h^n - s_h^n T_h^n\right) + h_{e,h}^n + \boldsymbol{h}_h^n \cdot \partial_t^n \boldsymbol{u}_h\right) \mathrm{d}x \\ &\leq \int_\Omega \left(C_6(|p_h^n|^2 + |T_h^n|^2) + C_7 + \frac{1}{2}|\partial_t^n \boldsymbol{u}_h|^2\right) \mathrm{d}x, \end{aligned} \tag{5.19}$$

where $C_6$ and $C_7$ are two real positive constants such that $C_6 = \max\left(\frac{C_1 C_5}{2}, C_1 C_4\right)$ and $C_7 = \frac{C_1 C_5}{2} + C_2 + \frac{C_3^2}{2}$.
Now, using the fact that $\mathbb{M}$ is a real symmetric matrix, we have

$$\lambda_{min} \|(p_h^n, T_h^n)\|_2^2 \leq \begin{bmatrix} p_h^n & T_h^n \end{bmatrix} \mathbb{M} \begin{bmatrix} p_h^n \\ T_h^n \end{bmatrix} \leq \lambda_{max} \|(p_h^n, T_h^n)\|_2^2, \tag{5.20}$$

where $\lambda_{min}$ and $\lambda_{max}$ are respectively the minimum and the maximum eigenvalues of $\mathbb{M}$.
Now, let us define the function $H : \mathbb{R} \to \mathbb{R}$ by

$$H(p_h^n) := \rho(p_h^n) g(p_h^n) - p_h^n \quad \text{with} \quad g(p_h^n) := \int_0^{p_h^n} \frac{1}{\rho(\zeta)}\, d\zeta.$$

We have that $H(p_h^n) \geq 0$. Using Assumptions **(A1)** and **(A4)**, together with inequality (5.20) and the fact that $H(p_h^n) \geq 0$, we deduce from the definition of $E_h^n$ that

$$E_h^n \geq \frac{1}{2}\lambda_{min} \|(p_h^n, T_h^n)\|_2^2 + \rho \phi_* e_h^n.$$

This leads to the following lower bound:

$$C_0(|p_h^n|^2 + |T_h^n|^2 + e_h^n) \leq E_h^n, \tag{5.21}$$

where $C_0 = \min\left(\frac{1}{2}\lambda_{min}, \rho\phi_*\right) > 0$ is a positive constant. Employing inequalities (5.19) and (5.21) in equation (5.15), we obtain

$$\begin{aligned} y^{N_T} &\leq y^0 + \delta t \sum_{n=1}^{N_T} \int_\Omega b \left(E_h^n + \frac{m_0}{2}|\partial_t^n \boldsymbol{u}_h|^2 - \operatorname{sgn}(p_h^n - p_h^{n-1})\phi_0 \gamma(p_h^n)^2\right) \mathrm{d}x \\ &\quad + \delta t \sum_{n=1}^{N_T} \int_\Omega \left(C_7 + \frac{1}{2}|\partial_t^n \boldsymbol{u}_h|^2 + b \operatorname{sgn}(p_h^n - p_h^{n-1})\phi_0 \gamma(p_h^n)^2\right) \mathrm{d}x \\ &= a^{N_T} + b \sum_{n=1}^{N_T} y^n, \end{aligned} \tag{5.22}$$

where $b = \delta t \max\left(\frac{C_6}{C_0}, 1\right)$ and

$$a^{N_T} = y^0 + \delta t N_T\, C_7 |\Omega| + \delta t \sum_{n=1}^{N_T} \int_\Omega \left(\frac{1}{2}|\partial_t^n \boldsymbol{u}_h|^2 + b \operatorname{sgn}(p_h^n - p_h^{n-1})\phi_0 \gamma(p_h^n)^2\right) \mathrm{d}x.$$

We now apply the discrete Gronwall lemma to (5.22). Since $b$ is constant and non-negative, it follows that

$$y^{N_T} \leq a_\theta \prod_{n=1}^{N_T}(1+b) = a_\theta(1+b)^{N_T},$$

where $\theta \in S(1, N_T) = \{k \text{ where } y^K(\prod_{j=1}^{k-1}(1+b_j))^{-1} \text{ is maximized in}\{1,\dots,N_T\}\}$.

Hence, there exists a constant $C > 0$ such that

$$\int_\Omega \left( E_h^n + \frac{m_0}{2}|\partial_t^n \boldsymbol{u}_h|^2 - \operatorname{sgn}(p_h^n - p_h^{n-1})\phi_0\gamma\,(p_h^n)^2 \right) \mathrm{d}x \leq C \quad \text{for all } n = 1,\dots,N_T. \tag{5.23}$$

Therefrom, from the assumption that $\phi_0\gamma$ is small, we deduce that $E_{\mathscr{D}} \in L^\infty(0, t_F, L^1(\Omega))$ and $\partial_t \boldsymbol{u}_{\mathscr{D}} \in L^\infty(0, t_F, L^2(\Omega))$. Furthermore, using the lower bound (5.21), we get that $p_{\mathscr{D}} \in L^\infty(0, t_F, L^2(\Omega))$, $T_{\mathscr{D}} \in L^\infty(0, t_F, L^2(\Omega))$ and $e_{\mathscr{D}} \in L^\infty(0, t_F, L^1(\Omega))$. Moreover, by the definition of $E_h^n$, and in particular the presence of the term involving $\epsilon(\boldsymbol{u}_h^n)$, it follows that $\epsilon(\boldsymbol{u}_{\mathscr{D}}) \in L^\infty(0, t_F, L^2(\Omega))$ and thus $\boldsymbol{\nabla}_h \boldsymbol{u}_{\mathscr{D}} \in L^\infty(0, t_F, L^2(\Omega))$. Consequently, we conclude that $\boldsymbol{u}_{\mathscr{D}} \in L^\infty(0, t_F, H^1(\Omega))$.
Given that $E_{\mathscr{D}} \in L^\infty(0, t_F, L^1(\Omega))$, $\partial_t \boldsymbol{u}_{\mathscr{D}} \in L^\infty(0, t_F, L^2(\Omega))$ and $p_{\mathscr{D}}, T_{\mathscr{D}} \in L^\infty(0, t_F, L^2(\Omega))$, we deduce from inequality (5.13) and the source terms bounds (5.19) that

$$\frac{\delta t}{d}\sum_{n=1}^{N_T}\int_\Omega \frac{\mathbb{K}}{\mu}|\boldsymbol{\nabla}_h p_h^n|^2 + \frac{\delta t}{d}\sum_{n=1}^{N_T}\int_\Omega \frac{\lambda}{T_{\text{ref}}}|\boldsymbol{\nabla}_h T_h^n|^2 \,\mathrm{d}x + \frac{\delta t}{d}\sum_{n=1}^{N_T}\int_\Omega \overline{\rho}_h' \frac{p_h^n}{\rho_h^n}|\boldsymbol{\nabla}_h p_h^n|^2 \,\mathrm{d}x \leq C, \tag{5.24}$$

which implies $\boldsymbol{\nabla}_h p_{\mathscr{D}} \in L^2(0, t_F, L^2(\Omega))$ and $\boldsymbol{\nabla}_h T_{\mathscr{D}} \in L^2(0, t_F, L^2(\Omega))$. Finally, we obtain the estimates (5.12). □

# 6 Numerical experiments

In this section, we present some numerical experiments associated to the proposed numerical scheme. To solve the nonlinear system of equations (4.5), (4.7) and (4.11), we employ the Newton method to "almost" convergence (the Newton tolerance is set to $10^{-10}$).

We consider a one-dimensional homogeneous porous medium of length $L$ . The initial porosity is set to $\phi_0 = 0.2$ and the constant absolute permeability is $\mathbb{K} = 10^{-12}m^2$. The gravitational effects are not taken into account in the numerical tests. We consider the same simulation parameters as in [14] and they are reported in the following table.

| Quantity | Symbol | Value | Unit |
|---|---|---|---|
| The Volumetric skeleton thermal dilatation coefficient | $\alpha_s$ | $1.5 \times 10^{-5}$ | $K^{-1}$ |
| Biot's coefficient | $b$ | 0.65 | – |
| Thermal Conductivity | $\lambda$ | 2 | W $m^{-1}K^{-1}$ |
| Poisson coefficient | $\nu$ | 0.15 | – |
| Young modulus | $E$ | $40.10^9$ | $Pa$ |
| Bulk modulus | $K_s$ | $\frac{E}{2(1+\nu)(1-2\nu)}$ | $Pa$ |
| Biot modulus | $N$ | $\frac{K_s}{(b-\phi^0)(1-b)}$ | $Pa$ |
| Skeleton volumetric heat capacity | $C_s$ | $2.10^6$ | J$m^{-3}K^{-1}$ |
| Reference temperature | $T_{\text{ref}}$ | 300 | $K$ |
| Reference pressure | $p_{\text{ref}}$ | $10^5$ | $Pa$ |
| The Volumetric thermal dilatation coefficient | $\alpha_\phi$ | $(b-\phi^0)\alpha_s$ | $K^{-1}$ |
| Average fluid skeleton specific density | $m_0$ | 0 | Kg $m^{-3}$ |

Table 1: Material properties.

### 6.1 Test Case with Exact Solutions

First, we analyse the numerical convergence of our scheme for the system of equations 2.1 using the following analytical solution:

$$p(x,t) = e^{-t}\sin(\pi x) + p_{\text{ref}}, \quad T(x,t) = T_{\text{ref}} - e^{-t}\sin(\pi x) \quad \text{and} \quad u(x,t) = 10^{-5}e^{-t}x(x-L)$$

on the domain $\Omega = (0,1)$ and time interval $(0, t_F)$ with $t_F = 1s$. Dirichlet boundary conditions are imposed for $p$, $T$, and $u$, and the source terms $h_m$, $h_e$, and $h$ are computed from the analytical solution using the parameters from Table 1. We consider a small constant time step $\delta t = 10^{-4}$. Moreover, the density of the fluid is given by

$$\rho(p) = \rho_{\text{ref}}(1 + c_{\text{ref}}(p - p_{\text{ref}})),$$

where $\rho_{\text{ref}} = 1000$ Kg $m^{-3}$ is the reference density and $c_{\text{ref}} = 10^{-6}Pa^{-1}$ is the compressibility coefficient. The fluid viscosity is set to $\mu = 10^{-3}$ Pa s. The fluid-specific entropy is given by

$$s(p,T) = C_f \ln\left(\frac{T}{T_{\text{ref}}}\right) - \left(\frac{1}{\rho_{\text{ref}}}\right)\ln\left(\frac{p}{p_{\text{ref}}}\right),$$

where $C_f = 1000\ J.Kg^{-1}.K^{-1}$ is the fluid specific heat capacity.

The relative $L^2$ space-time errors for $p$, $T$, and $u$ are presented in Figure 2 as functions of the number of mesh elements $N_x$.

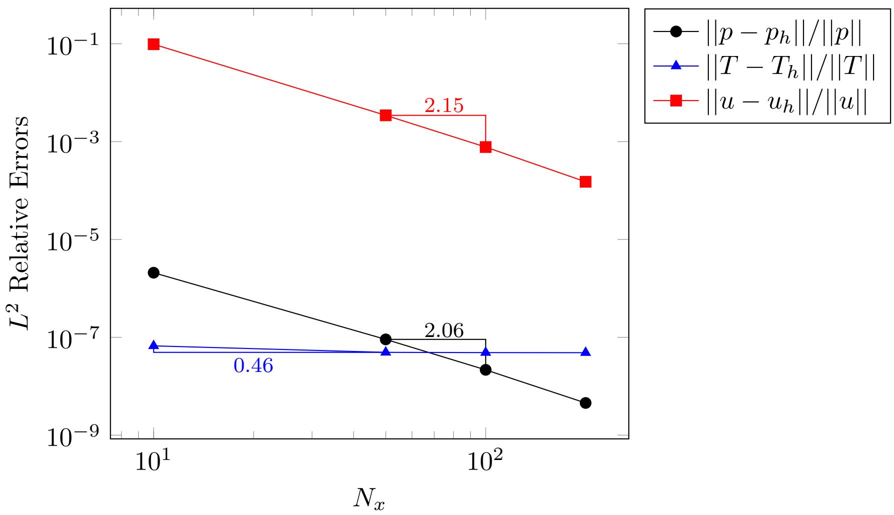


Figure 2: Relative $L^2$ errors for the pressure $p$, the temperature $T$, and the displacement $u$.

Figure 2 shows the relative $L^2$ space-time errors for the primary unknowns: fluid pressure $p$, fluid temperature $T$ and skeleton displacement $u$, as a function of the number of spatial mesh elements $N_x$. The relative $L^2$ space-time error is defined, for example, for the pressure, as

$$\frac{\|p - p_h\|_{L^2(\Omega, L^2(0,t_F))}}{\|p\|_{L^2(\Omega, L^2(0,t_F))}} = \frac{\left(\int_0^{t_F}\int_\Omega (p - p_h)^2 \,\mathrm{d}x\mathrm{d}t\right)^{1/2}}{\left(\int_0^{t_F}\int_\Omega p^2 \,\mathrm{d}x\mathrm{d}t\right)^{1/2}}.$$

Similar expressions are used for the variables $T$ and $u$. This figure highlights the different convergence behaviors, which are consistent with those reported for incompressible fluids in [13]: the pressure and displacement exhibit approximately second-order convergence, while the temperature shows a slower convergence rate of about 0.5. Moreover, the results are comparable to those observed for a compressible flow in fractured porous media [14], where the convergence rate of the model is approximately 1.5. Overall, these results demonstrate the accuracy and robustness of the proposed numerical scheme.

## 6.2 Dirichlet Boundary Conditions

We consider a one-dimensional homogeneous porous medium of length $L = 10$ m. We fix the initial pressure, temperature, and displacement field to $p^0 = 10^5 Pa$, $T^0 = 300K$, and $u^0 = 10^{-6}m$, respectively. Dirichlet boundary conditions are imposed on the pressure, with $p = 4 \times 10^5 Pa$ on the left boundary and $p = 10^5 Pa$ on the right boundary. For the temperature, we fix $T = 285K$ on the left boundary and $T = 300K$ on the right boundary. The displacement field satisfies homogeneous Dirichlet boundary conditions, representing a waterproof sample. This configuration is particularly relevant as it enables the investigation of the risk associated with pressure buildup resulting from the restriction of fluid outflow. In addition, the source terms $h_m$, $h_e$, and $h$ are set to 0.

We consider a uniform spatial mesh ($N_x = 100$ elements) and let $t_F = 1$ day be the final simulation time with $\delta t = 10^{-3}s$ the constant time step.

In Figure 3, we show the behavior of our numerical solution through the porous medium at the final simulation time $t = 1$ day. More precisely, we displayed the fluid pressure (left), fluid temperature (middle) and skeleton displacement (right). We note that the pressure decreases rapidly near the left boundary and stabilizes further into the domain. The temperature increases before reaching a nearly constant value, while the displacement initially increases in the first cells, reaching a maximum around $8.10^{-5} - 9.10^{-5}m$, and then decreases further into the domain. We observe that negative displacement values were generated; this is due to the fixed boundaries on both ends of the domain and unrealistic data in this test case. These behaviors are consistent with the applied boundary conditions and the coupled thermo-poroelastic nature of the system, demonstrating the strength of our approach.

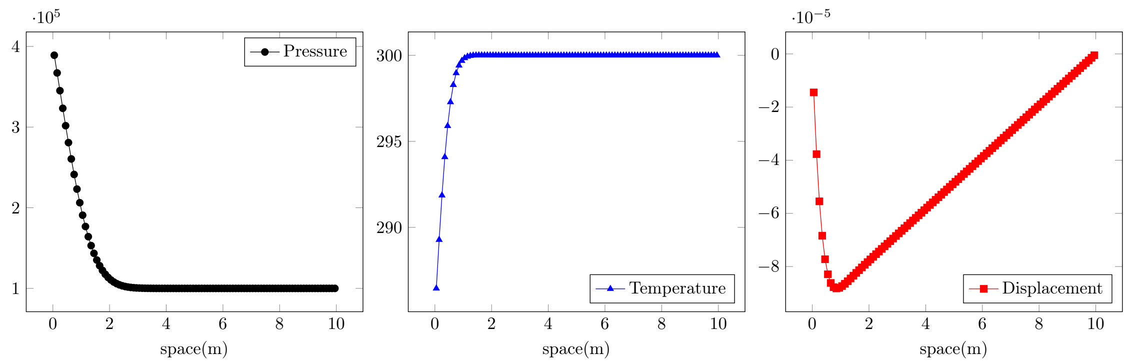


Figure 3: Solution for $N_x = 100$ spatial elements at $t = 1$ day. Fluid pressure (left), fluid temperature (middle), and skeleton displacement (right).

In Figure 4, we represent the evolution of the numerical solution over time, from $t = 2$ days to $t = 100$ days, as a function of the spatial domain. We observe that the fluid pressure increases over time and gradually approaches a steady, nearly linear profile. An analogous behavior is observed for the temperature, which stabilizes progressively over time. In contrast, the displacement decreases and develops a wave-like profile at later times.

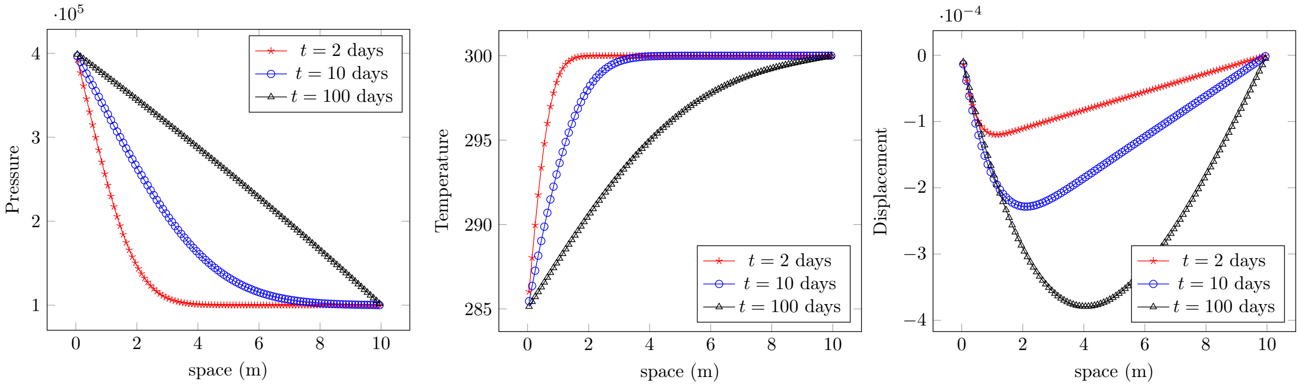


Figure 4: Profile of the numerical solution for $N_x = 100$ spatial elements at different time values. *Left*: fluid pressure, *middle*: fluid temperature, *right*: skeleton displacement.

### 6.3 Influence of the displacement

In this section, we investigate the influence of the skeleton displacement on the numerical solution. We consider three cases:

1. **No displacement ($\boldsymbol{u} = 0$):** we assume that the skeleton undergoes no displacement. As a result, the system of equations (2.1) contains only the fluid mass conservation equation and the energy balance equation. In addition, we define the porosity as $\phi = \phi(p, T)$ and the volumetric skeleton entropy as $S_s = S_s(p, T)$.

2. **Initial displacement $\boldsymbol{u}^0 = 0$:** We consider the system of equations (2.1) where the initial displacement is equal to zero.

3. **Initial displacement $\boldsymbol{u}^0 = 10^{-6}$:** We consider the system of equations (2.1) where the initial displacement is equal to $10^{-6}$ m.

Moreover, we consider the same parameters and boundary conditions mentioned in Section 6.2.

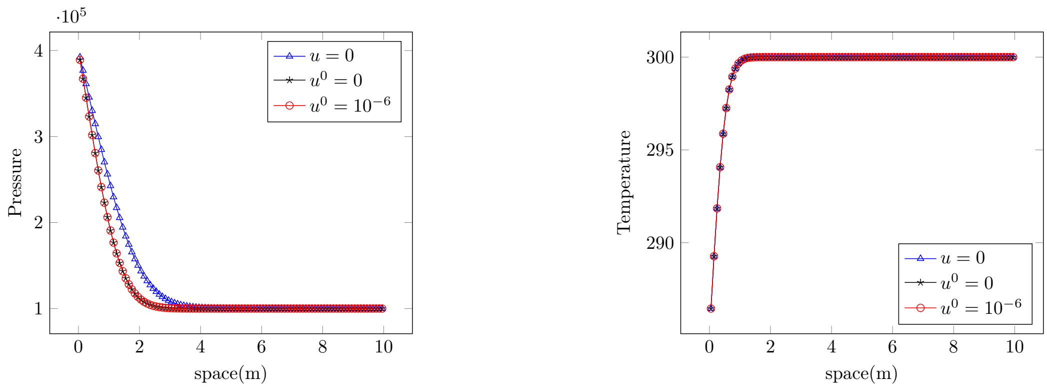


Figure 5: Numerical solution for diffrent cases depending on the skeleton displacement at $t = 1$ day. *Left*: fluid pressure and *right*: fluid temperature.

Figure 5 illustrates the numerical solution (fluid pressure and temperature) under three cases : (1) with no displacement, (2) with an initial displacement field $\boldsymbol{u}^0 = 0$ m, and (3) with $\boldsymbol{u}^0 = 10^{-6}$ m, for $N_x = 100$ spatial elements at $t = 1$ day. We observe that the behaviors of the temperature for these three configurations are similar. It shows, in particular, that variations of the displacement $\boldsymbol{u}$ do not affect the evolution of the temperature variable. However, the pressure is slightly higher when the displacement is neglected in the model, whereas in the other case, the variation of the initial displacement does not affect the evolution of the fluid pressure.

## 6.4 Influence of the compressibility

In this section, we analyze the influence of compressibility on our numerical solution. We consider three cases:

1. **Incompressible fluid:** In this case, we suppose that the fluid is incompressible with a constant density $\rho = 1000$ Kg $m^{-3}$ and we set the fluid viscosity to $\mu = 10^{-3}$ Pa s. The fluid-specific entropy is given by $s(T) = C_f \ln\left(\frac{T}{T_{\text{ref}}}\right)$.

2. **Weakly compressible fluid:** The density of the fluid is given by $\rho(p) = \rho_{\text{ref}}(1 + c_{\text{ref}}(p - p_{\text{ref}}))$ where $\rho_{\text{ref}} = 1000$ Kg $m^{-3}$ is the reference density and $c_{\text{ref}} = 10^{-6} Pa^{-1}$ is the compressibility coefficient. In addition, the fluid viscosity is set to $\mu = 10^{-3}$ Pa s. The fluid-specific entropy is given by $s(p, T) = C_f \ln\left(\frac{T}{T_{\text{ref}}}\right) - \left(\frac{1}{\rho_{\text{ref}}}\right) \ln\left(\frac{p}{p_{\text{ref}}}\right)$.

3. **Perfect gas case:** The density of the fluid is given by $\rho(p) = M_g \frac{p}{RT_{\text{ref}}}$ where $M_g = 2.01568\ 10^{-3}$ Kg.mol$^{-1}$ is the molar mass of the hydrogen and $R = 8.3149$ J.mol$^{-1}$.K$^{-1}$ is the perfect gas constant. In addition, the fluid viscosity is set to $\mu = 9 \times 10^{-5}$ Pa s. The fluid-specific entropy is given by $s(p, T) = C_f \ln\left(\frac{T}{T_{\text{ref}}}\right) - R \ln\left(\frac{p}{p_{\text{ref}}}\right)$.

The parameters and boundary conditions used are consistent with those specified in Section 6.2.

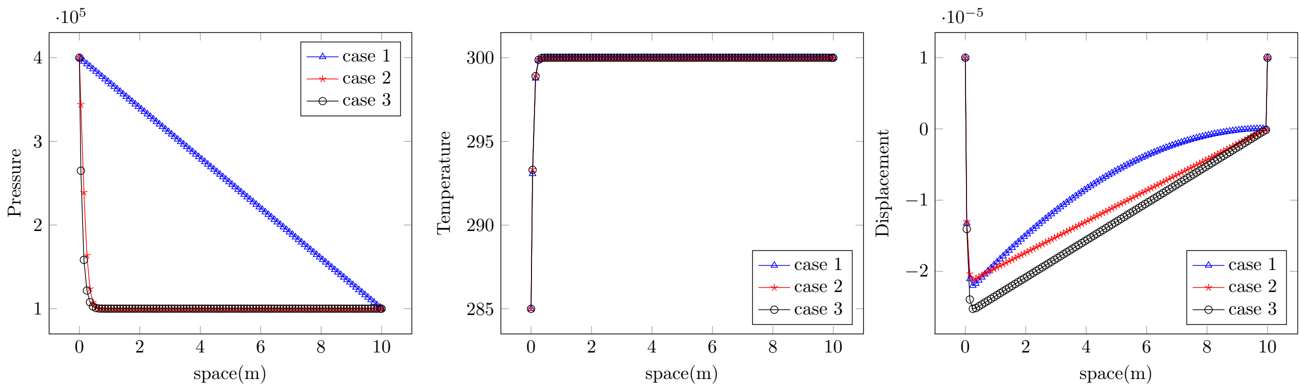


Figure 6: Numerical solution for different cases depending on the compressibility of the fluid at $t = 1$ hour using $N_x = 100$ spatial elements. *Left*: fluid pressure, *middle*: fluid temperature, and *right*: skeleton displacement.

In Figure 6, we show the behavior of the numerical solution under different cases depending on the compressibility of the fluid : case 1 (black curve) with an incompressible fluid, case 2 (red curve) with a weakly compressible fluid, and case 3 (blue curve) with a perfect gas. We observe that the pressure in the incompressible case is greater than in the compressible cases, where it is nearly the same. In contrast, the compressibility of the fluid does not affect its temperature, which stays similar in all cases. Finally, we observe that the skeleton displacement is greater for an incompressible fluid than a compressible one. Moreover, in the case of a weakly compressible fluid, the displacement exceeds that observed for a perfect gas.

### 6.5 Neumann Boundary Conditions

In this section, we consider the same parameters mentioned in Section 6.2 with different boundary conditions. We employ homogeneous Neumann boundary conditions for the pressure and temperature. For the displacement, we employ homogeneous Dirichlet on the left boundary and homogeneous Neumann on the right.

Figure 7 represents the evolution of the numerical solution over time, from day 1 to day 100, through the porous medium. We observe that, at each time, the fluid pressure decreases progressively when moving further into the domain. However, the temporal evolution reveals a crossover: at $t = 10$ and $t = 100$ days, the pressure is lower than at $t = 1$ day in the first cells of the domain (approximately $x \leq 2$ m), but becomes higher than the pressure at $t = 1$ day further into the domain. Moreover, at $t = 100$ days the pressure is lower than at $t = 10$ days in the first half of the domain, but is higher in the second half. This behavior reflects the progressive redistribution of the fluid, consistent with the imposed boundary conditions, where the pressure gradient is zero at both ends. The same behavior is observed for the fluid temperature, since identical boundary conditions are imposed for the thermal flow, leading to a similar redistribution process over time. Finally, for the displacement field, we observe that it increases both with time and along the spatial domain. This is a consequence of the boundary conditions: no displacement was imposed on the left of the domain, while a Neumann condition on the right allows displacement to accumulate and grow over time.

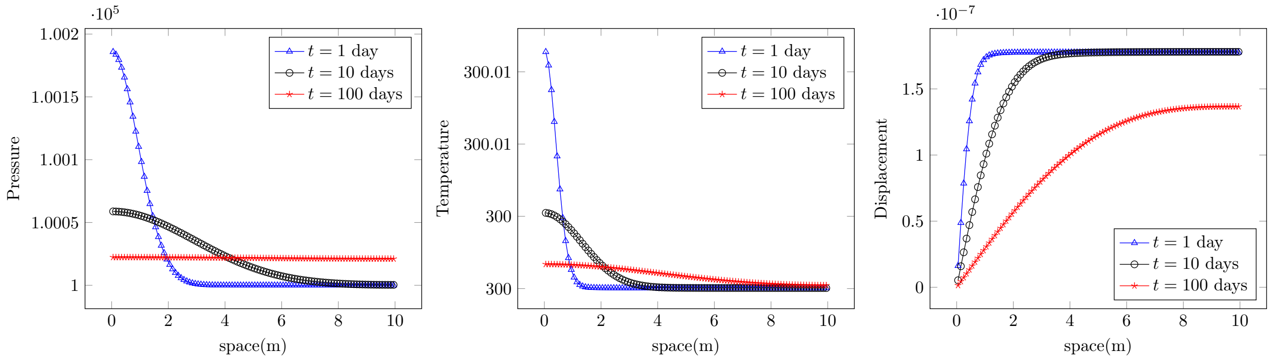


Figure 7: Numerical solution at different times using $N_x = 100$ spatial elements. *Left*: fluid pressure, *middle*: fluid temperature, and *right*: skeleton displacement.

# 7 Conclusion

In this work, we investigated discretizations that preserve energy estimates for a THM model describing compressible fluid flow in deformable porous media. We employed the finite volume method with two-point flux approximation for the spatial discretization, and the implicit Euler scheme for the discretization in time. Particular attention was given to the choice of the fluid density at the interface, where a non-classical definition was adopted to ensure the preservation of the energy estimates at the discrete level. Energy estimates were derived and presented at both the continuous and discrete levels. The proposed approach was then tested and validated through numerical experiments under different boundary conditions, and the influence of fluid compressibility was examined. The results confirmed the robustness and reliability of the method.

In future work, we aim to extend the model and discretization framework to the case of two-phase flow in deformable porous media, where additional unknowns and nonlinear couplings will pose new analytical and numerical challenges.

# Acknowledgments

This work has received funding from the Région Pays de la Loire. The second author gratefully acknowledges the support of the NASINE project (2023-2025), funded by the PULSAR Academy of Young Researchers

in Pays de la Loire.

## References


[1] B. Amaziane, M. El Ossmani, and Y. Zahraoui, *Convergence of a tpfa finite volume scheme for nonisothermal immiscible compressible two-phase flow in porous media*, Computers & Mathematics with Applications, 165 (2024), pp. 118–149.

[2] M. Bendahmane, Z. Khalil, and M. Saad, *Convergence of a finite volume scheme for gas–water flow in a multi-dimensional porous medium*, Mathematical Models and Methods in Applied Sciences, 24 (2014), pp. 145–185.

[3] M. A. Biot, *General theory of three-dimensional consolidation*, Journal of applied physics, 12 (1941), pp. 155–164.

[4] M. A. Biot and D. G. Willis, *The elastic coefficients of the theory of consolidation*, Journal of Applied Mechanics, 24 (1957), pp. 594–601.

[5] F. Bonaldi, K. Brenner, J. Droniou, and R. Masson, *Gradient discretization of two-phase flows coupled with mechanical deformation in fractured porous media*, Computers & Mathematics with Applications, 98 (2021), pp. 40–68.

[6] K. Bouadjila, A. Mokrane, A. S. Saad, and M. Saad, *Numerical analysis of a finite volume scheme for two incompressible phase flow with dynamic capillary pressure*, Computers & Mathematics with Applications, 75 (2018), pp. 3614–3631.

[7] H. Brezis, *Functional analysis, Sobolev spaces and partial differential equations*, Universitext, Springer, New York, 2011.

[8] G. Chavent and J. Jaffré, *Mathematical models and finite elements for reservoir simulation*, North Holland, 1986.

[9] D. S. Clark, *Short proof of a discrete gronwall inequality*, Discrete applied mathematics, 16 (1987), pp. 279–281.

[10] O. Coussy, *Poromechanics*, John Wiley & Sons, 2004.

[11] B. M. Dia, B. Saad, and M. Saad, *Modeling and simulation of partially miscible two-phase flow with kinetics mass transfer*, Mathematics and Computers in Simulation, 186 (2021), pp. 29–40.

[12] J. Droniou, R. Eymard, T. Gallouët, and R. Herbin, *A unified approach to mimetic finite difference, hybrid finite volume and mixed finite volume methods*, Mathematical Models and Methods in Applied Sciences, 20 (2010), pp. 265–295.

[13] J. Droniou, M. Laaziri, and R. Masson, *Thermodynamically consistent discretisation of a thermo-hydro-mechanical model*, in International Conference on Finite Volumes for Complex Applications, Springer, 2023, pp. 265–273.

[14] J. Droniou, M. Laaziri, and R. Masson, *Discretisations of mixed-dimensional thermo-hydro-mechanical models preserving energy estimates*, Journal of Computational Physics, 515 (2024).

[15] M. El-Shafie, *Hydrogen production by water electrolysis technologies: A review*, Results in Engineering, 20 (2023).

[16] R. Eymard, T. Gallouët, and R. Herbin, *Finite volume methods*, in Handbook of numerical analysis, Vol. VII, Handb. Numer. Anal., VII, North-Holland, Amsterdam, 2000, pp. 713–1020.

[17] I. B. Gharbia, J. Dabaghi, V. Martin, and M. Vohralík, *A posteriori error estimates for a compositional two-phase flow with nonlinear complementarity constraints*, Comput. Geosci., 24 (2020), pp. 1031–1055.

[18] M. Ghilani, M. Saad, et al., *Positivity-preserving finite volume scheme for compressible two-phase flows in anisotropic porous media: the densities are depending on the physical pressures*, Journal of Computational Physics, 407 (2020).

[19] T. H. Gronwall, *Note on the derivatives with respect to a parameter of the solutions of a system of differential equations*, Annals of Mathematics, 20 (1919), pp. 292–296.

[20] G. A. Holzapfel, *Nonlinear solid mechanics: a continuum approach for engineering science*, Kluwer Academic Publishers, 2002.

[21] A. Hussain, H. Emadi, S. R. Thiyagarajan, D. M. Fernandez, I. Ispas, and M. Watson, *Non-destructive cyclic analysis of sealing ability of well cement for seasonal underground hydrogen storage*, Applied Sciences, 14 (2024).

[22] E. Ohaeri, U. Eduok, and J. Szpunar, *Hydrogen related degradation in pipeline steel: A review*, International Journal of Hydrogen Energy, 43 (2018), pp. 14584–14617.

[23] W. Rudin, *Principles of Mathematical Analysis*, McGraw-Hill Publishing Company, 1976.

[24] B. Saad, *Modélisation et simulation numérique d'écoulements multi-composants en milieu poreux*, theses, Ecole Centrale de Nantes (ECN), Dec. 2011.

[25] B. Saad and M. Saad, *Study of full implicit petroleum engineering finite-volume scheme for compressible two-phase flow in porous media*, SIAM Journal on Numerical Analysis, 51 (2013), pp. 716–741.

[26] M. Saad, *Slightly compressible and immiscible two-phase flow in porous media*, Nonlinear Analysis: Real World Applications, 15 (2014), pp. 12–26.

[27] S. Q. Sun B., Zhang M. and et al, *Review on natural hydrogen wells safety*, Nature Communications 16, (2025).

[28] R. Tarkowski, *Underground hydrogen storage: Characteristics and prospects*, Renewable and Sustainable Energy Reviews, 105 (2019), pp. 86–94.

[29] K. Terzaghi, R. B. Peck, and G. Mesri, *Soil mechanics*, New York: John Wiley & Sons, (1996).

[30] A. Uliasz–Bocheńczyk and R. Wiśniowski, *Impact of hydrogen on cement slurry: A review*, Renewable and Sustainable Energy Reviews, 214 (2025).